PARALLELIZATION OF *IN VIVO*-LIKE ANTI-CANCER DRUG CONCENTRATION PROFILES ON TOP PLATFORM FOR TESTING DRUG EFFICACY ON TUMOUR SPHEROIDS

Master Thesis by

Koen Nijboer

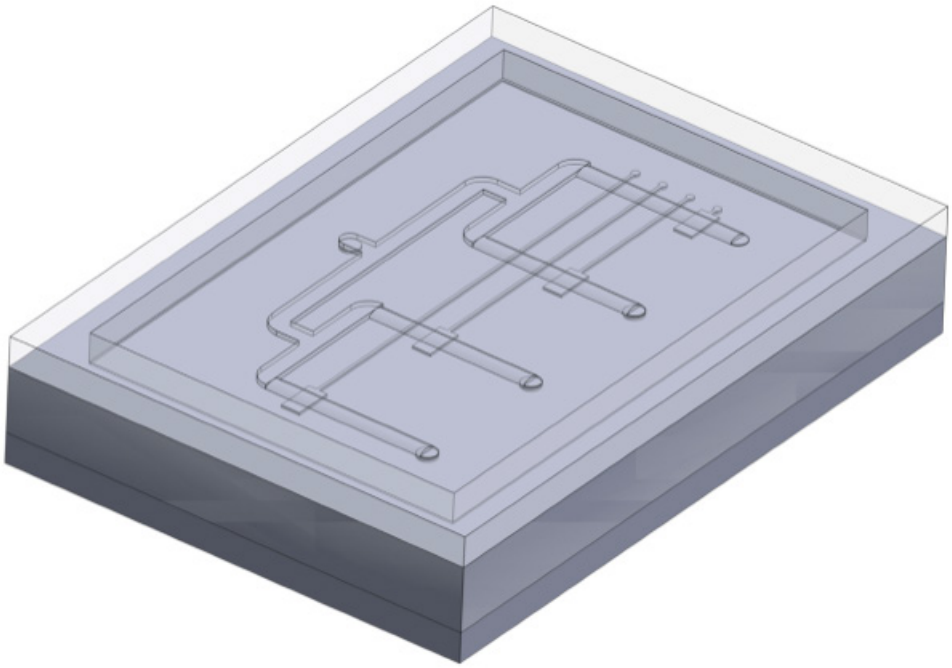

April 14, 2022

Student Koen Nijboer **Chair** BIOS Lab-on-a-Chip group | Faculty of Science and Technology | University of Twente, the Netherlands **Graduation Committee** Drs. J. Komen MD (Daily supervisor), E.G.B.M. Bossink (Daily supervisor), Prof.dr.ir. A. van den Berg (Committee chair), Dr. A.D. van der Meer (External member)

UNIVERSITY OF TWENTE.

BIOS Lab on a Chip group

Cover page image: Design of the Drug Distribution Chip (DDC) that was developed throughout this project, produced in SolidWorks.

Abstract

Cancer is one of the leading causes of death worldwide. Out of the treatment methods available for the treatment of cancer, chemotherapy is one of the most effective and is applied in approximately 30 % of cases. *In vitro* and *in vivo* models, used for testing the efficacy of anti-cancer drugs in the preclinical phase of the drug development regulatory pathway have several shortcomings, leading to a rate of gaining clinical approval for potential anti-cancer drugs of only 7%. *In vitro* 2D models do not fully recapitulate the *in vivo* tumour physiology and the static conditions under which testing is performed do not account for the pharmacokinetics inside the human body. Moreover, *in vivo* animal models have often proven to be insufficiently translatable to humans for testing new drugs on efficacy and safety. This generated a growing interest in more complex *in vitro* models that make use of Organ-on-Chip and 3D cell cultures.

In this project, an *in vitro*, microfluidic system is introduced, with which dynamic, *in vivo*-like, anti-cancer drug concentration profiles can be sequentially parallelized. One microfluidic chip was developed and used twice in the system. First, to generate the dynamic concentration profile, and subsequently for sequential parallelization of the concentration profiles over three microfluidic channels. Colorectal tumour spheroids were integrated in the microfluidic channels to form a Tumour-Spheroid-on-Chip model. The ability of the system to steadily parallelize a dynamic concentration profile was successfully demonstrated, using fluorescein as a model drug. Additionally, it was proven that the spheroids were able to grow on chip, during sequential parallelization of cell culture medium. Finally, three tumour spheroids were placed in series in the three separate microfluidic channels. The total of nine spheroids were exposed to the *in vivo* oxaliplatin concentration profile, where growth inhibition was observed for all spheroids. A proposed method for further upscaling of the system was given, where the microfluidic chips can be integrated on the Translational-Organ-on-Chip platform to be able to simultaneously test up to two different *in vivo* anti-cancer drug concentration profiles over a total of 18 tumour spheroids.

Samenvatting

Kanker is een van de grootste doodsoorzaken wereldwijd. Uit alle behandelmethodes die er beschikbaar zijn voor kanker is chemotherapie een van de meest effectieve en wordt deze behandelmethode in 30 % van de gevallen toegepast. *In vitro* en *in vivo* modellen, die worden gebruikt in de preklinische fase van geneesmiddelontwikkeling, hebben enkele tekortkomingen, wat ertoe leidt dat maar 7 % van de potentiële chemotherapieën wordt goedgekeurd. *In vitro* 2D modellen zijn niet in staat de tumor fysiologie voldoende na te bootsen en de statische condities waaronder de testen worden uitgevoerd houden geen rekening met de farmacokinetiek in het lichaam. Bovendien zijn de *in vivo* diermodellen niet altijd voldoende vertaalbaar naar mensen om potentiële, nieuwe chemotherapieën te testen op effectiviteit en veiligheid. Dit heeft een interesse gegenereerd in meer complexe *in vitro* modellen, die gebruik maken van orgaan-op-een-chip technologie en 3D celculturen.

In dit project wordt een systeem geïntroduceerd waarmee dynamische, *in vivo* representatieve, concentratie profielen van chemotherapieën sequentieel geparallelliseerd kunnen worden. Hiervoor is een microfluïdische chip ontwikkeld, die twee keer in het systeem wordt gebruikt. Eerst om een dynamisch concentratie profiel te genereren en vervolgens om het concentratie profiel sequentieel te kunnen parallelliseren over drie microfluïdische kanalen. Colorectale tumor spheroids werden geïntegreerd in de microfluïdische kanalen om zo een Tumor-Spheroid-op-Chip model te vormen. De mogelijkheid om met het systeem dynamische concentratie profielen te parallelliseren werd succesvol aangetoond met fluoresceïne, dat als model werd gebruikt. Daarnaast werd aangetoond dat de spheroids kunnen groeien in de chip, wanneer ze sequentieel aan celkweekmedium werden blootgesteld. In het laatste experiment werden er drie spheroids in serie geplaats per chip. De, in totaal negen, spheroids werden blootgesteld aan het *in vivo* oxaliplatine concentratie profiel, waarna er groeiremming in alle spheroids werd vastgesteld. Ten slotte werd een manier om het systeem verder op te schalen voorgesteld, waarbij de microfluïdische chips geïntegreerd kunnen worden op het Translational-Organ-on-Chip platform. Hiermee kunnen er twee verschillende *in vivo* concentratie profielen van chemotherapieën simultaan getest worden op een totaal aantal van achttien spheroids.

Contents

1 Introduction

This thesis is focused on the development of an *in vitro* system for parallel testing of dynamic *in vivo*-like anti-cancer drug concentrations on colorectal tumour spheroids.

1.1 Cancer and anti-cancer drugs

Cancer is one of the leading causes of death among the world's population. It accounts for roughly one in six deaths worldwide, with nearly 10 millions deaths caused by cancer in 2020 [1]. Cancer is characterized by the transformation of healthy cells into diseased, abnormal cells that divide uncontrollably [2]. This way, tumours are formed, which grow over time and can cause damage to or destroy healthy body tissue. Depending on the type of cancer and its stage, the general health of the patient and the patients preferences, different treatment methods are applied [2]. Out of all these treatment methods, chemotherapy is one of the most effective ways to treat cancer and approximately 30 % of cancer patients receive this treatment [3], [4].

1.2 Current drug testing methods

The entire process that a new drug has to go through in order to reach the market consist of four different phases; drug discovery, the preclinical phase, clinical development and the post-market surveillance. After drug discovery, the first phase of testing is defined as the preclinical phase, during which drug efficacy, toxicity, pharmacokinetics and pharmacodynamics are studied in *in vitro* and *in vivo* animal models.

1.2.1 *In vitro* models

In vitro models replicate specific parts and functions of the human body and can be used to study cell behaviour and response outside of the human body [5]. They are the starting point in medical and biological research. Often, simplified models, comprised of 2D monolayers of immortalized cells, are used for recapitulating *in vivo* behaviour due to easy manipulation [6]. *In vitro* drug testing methods currently used for investigating potential anti-cancer drugs, as part of the preclinical phases, are performed in 2D under static conditions [7]. However, drug testing in these conditions is not physiologically representative for the *in vivo* situation, as the tumour microenvironment is not recapitulated [8]. Moreover, the static conditions used in current drug testing methods do not correspond with the dynamic drug concentrations, or pharmacokinetics, inside the human body when administering a drug. The imperfect predictability of the currently used *in vitro* models and the poor translation between the *in vitro* and *in vivo* models likely contribute to a rate of gaining clinical approval for potential anti-cancer drugs of only 7% [9]. This is significantly lower than the rate for drugs treating other diseases [9].

1.2.2 *In vivo* models

In vivo models are used for studying cell behaviour and response inside of a living organism. This can be done in animals or in humans during clinical trials. The *in vivo* animal models that are mostly used are cell line-derived xenograft (CDX) models, where cancer cell lines from patients are implanted in immunodeficient mice. These models have been dominantly used for gaining insights into human biology, disease, pharmacology and toxicology. However, they have often proven to be insufficiently translatable to humans for testing new therapies, drugs on efficacy and safety. This is due to passaging of cells under conditions that not recapitulate the natural tumour microenvironment [10]. It is clear that models with higher translation to the clinic are needed. Therefore, in 2016 the The National Cancer Institute (NCI) announced a new repository of cancer models, to (partly) replace the current NCI-60 drug test methodology, by focusing on patient derived xenograft (PDX) [11]. For PDX models, tumor tissue is implanted in mice, for better recapitulation of the cancer microenvironment, compared to CDX models [12]. Next to the increase in interest in PDX models, the shortcomings of currently used animal models and *in vitro* 2D models generated a growing interest in more complex *in vitro* models that make use of Organ-on-chip and 3D cell cultures. [6]

1.2.3 Cancer-on-chip models

Over the past years microfluidics has emerged as a better alternative for the currently used 2D *in vitro* drug testing methods [13]. Microfluidics facilitates high-throughput experiments on a small surface area, with minimal consumption of substances and the possibility for parallelization with multi-channel designs [14]. A major advantage of microfluidics is the possibility for complex 3D cell cultures to be integrated in the microfluidic channels, to form an Organ-on-chip (OoC) model. These combine the flow of medium, to facilitate oxygen and nutrient supply to 3D cell cultures, thereby mimicking vascular perfusion in the human body [13]. OoC models recapitulate tissue- and organ-level physiology to a degree that is not possible with 2D culture systems [15].

To study the response of a tumour to anti-cancer drugs, tumour spheroids can be integrated in a microfluidic system to form a Tumour-Spheroid-on-Chip (TSoC) model. Tumour spheroids are 3D cell aggregates of a certain cancer cell line, with sizes typically ranging from 100 to 1000 µm in diameter. They form through self-assembly when cultured in an environment that prevents the cells from attaching to a flat surface. Spheroids have several great benefits over the 2D cell cultures used in drug screening today. They better represent the heterogeneous *in vivo* structure of tissue compared to 2D cell cultures, as they possess important physiological parameters that are displayed in *in vivo* tumours, including cell-cell interaction and similar mechanical tissue properties. Moreover, spheroids display a nutrient and drug gradient from outside the spheroid to the core, posses growth kinetics and show gene expression levels similar to *in vivo* tumours. [16], [17], [18]

A useful application of this TSoC model and microfluidics in the field of drug testing is its ability to create dynamic drug concentration profiles of certain substances or drugs on chip and supply those to the tumour spheroids. This facilitates replicating the *in vivo* drug distribution, or pharmacokinetics, thereby increasing the physiological relevance of *in vitro* drug testing. In combination with the previously mentioned advantages of microfluidics for high-throughput drug screening, these TSoC models can be used for more patient specific treatment by testing a variety of different anti-cancer drugs and different dosing schemes.

The general drug concentration profile that is observed *in vivo* is shown in figure 1. After administration of a drug, there is first an increase in concentration due to absorption of the drug. After a peak concentration is reached, the concentration gradually decreases over time due to excretion of the drug. The specific profile is different for different types of drugs and is described by various pharmacokinetic parameters [19]. Important parameters are the peak concentration of a drug after administration and the time to reach that peak, which are given by C_{max} and T_{max} respectively, the time it takes for the concentration to reduce by 50%, which is given by the plasma half-life, $T_{1/2}$, and the area under the curve (AUC), that gives the integral of the entire concentration-time graph [19]. The AUC is a relevant pharmacokinetic parameter for drug exposure as it represents the total drug exposure across time [20]. Recently, several attempts have been made to establish dynamic drug concentrations on chip [21], [22], [23], [24]. However, the systems developed in that research still have limitations, where one important limitation is parallelization of the system.

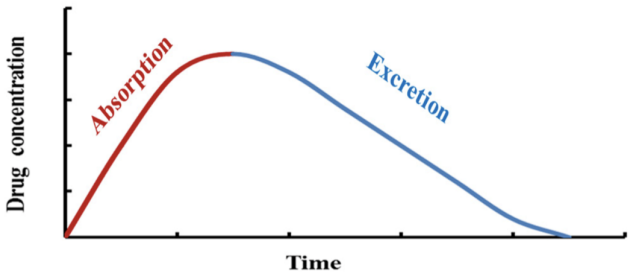

Figure 1: General *in vivo* drug concentration versus time curve. [25]

1.3 The importance of parallelization of cancer-on-chip systems

High-throughput drug screening can be easily achieved with 2D drug screening techniques. However, upscaling is still a challenge for more complex microfluidic systems [23], [26]. The inability of most of the more complex *in vitro* models today to perform medium- to high-throughput testing requires multiple models to provide sufficient replicas. However, this makes it hard or even impossible to create appropriate controls for validation of the obtained results [27]. Development of high-throughput *in vitro* models could finally lead to wide-scale use of OoC technology in the preclinical drug testing phase. Therefore, parallelization, while maintaining the ability to administer dynamic drug concentrations, is the key focus of this project.

1.4 State-of-the-art

1.4.1 Existing solutions

Recently, several attempts were made to generate dynamic drug concentration profiles on microfluidic chip in a parallel manner. In every research, a different approach was used to achieve this.

Lohasz et al presents an approach that makes use of gravity to achieve a dynamic drug concentration profile on chip. They designed a tubing-less microfluidic chip, shown in figure 2, with two reservoirs on chip that come together via an asymmetric Y-junction. The channels coming together from the reservoirs both have a different hydraulic resistance, as one has a significantly smaller diameter. The Y-junction allows for mixing the two substances from the reservoirs. The mixed fluid flows past 6 microtissues that are integrated in the microfluidic channel. This way, upon tilting the chip, different rates of mixing can be realized. Disadvantages of this system are the limited range in drug concentrations that can be realized on chip, the lack of a constant flow rate over time as culture medium needs to be refreshed during experiments and the inability to precisely replicate dynamic concentration profiles on chip. [22]

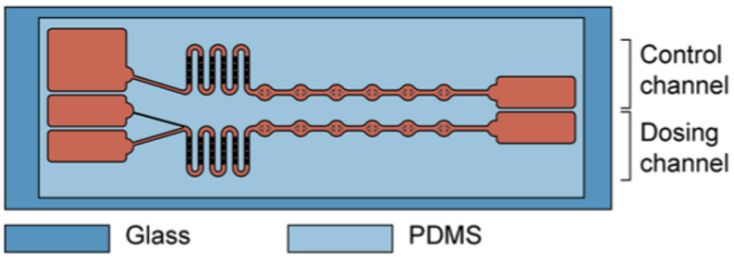

Figure 2: Microfluidic chip design by Lohasz et al. [22]

An interesting approach to apply physiologically relevant pharmacokinetic drug profiles on chip was introduced by Guerrero et al [24]. They make use of two syringe pumps, where one is filled with cell media and one is filled with an anti-cancer drug, to supply a dynamic drug concentration profile to a cell culture, that is placed in a culture well inside a microfluidic channel. A similar approach was later used by Komen et al [28]. The microfluidic chip design used by Guerrero et al consists of two inlet channels that come together in a mixing channel through a Y-junction, where the mixed fluid then continues to flow through a culture well and leaves the chip at the outlet. An overview of the setup is shown in figure 3. The drug pharmacokinetic profiles for the drugs used in this research were based on published animal or human pharmacokinetics data. With modeling software (MATLAB), the flow rates of both syringe pumps were programmed, where the flow rate applied to the cell culture was constant. The disadvantage of this system is the lack of parallelization and difficulty for further parallelization.

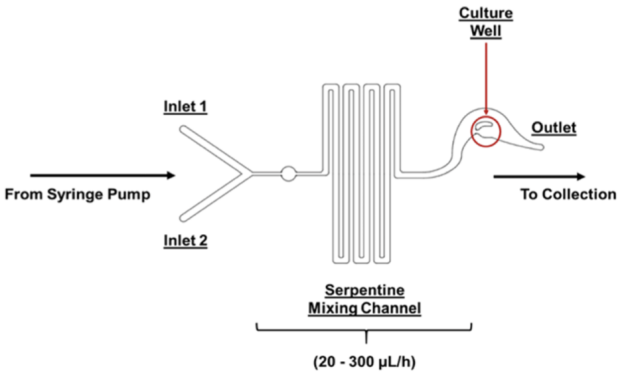

Figure 3: Schematic overview of the microfluidic chip design by Guerrero et al. [24]

Petreus et al introduces a relatively simple chip design that consists of one microfluidic channel in which eight Matrigel-encapsulated colorectal tumour spheroids were integrated. To supply a dynamic drug concentration profile, they used commercially available equipment, including a 10/11 port MUX distributor valve and pressure controller from Elvesys and digital, thermal flow sensors from Elveflow. With the flow sensor and the pressure controller, a constant flow rate could be maintained over time. The complete setup and the microfluidic chip used in the setup are shown in figure 4.

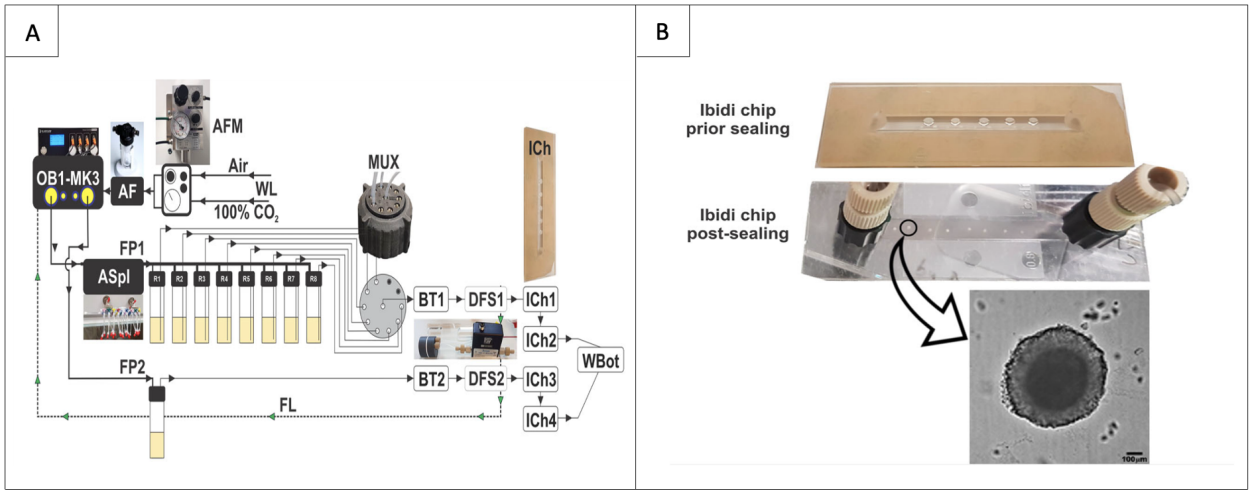

Figure 4: A) An overview of the setup used by Petreus et al. Where AFM = airflow mixer, OB1-MK3 = piezo pump, AF = air filter, WL = wall lines, FP1 = flow path 1, ASpl = air splitter, MUX = 10/11 port distributor, BT = bubble trap, DFS = digital flow sensor, ICh = Ibidi microfluidic chip and FL = feedback loop. B) The microfluidic chip used in the setup. [23]

The eight reservoirs were each filled with different concentrations of the two drugs, Irinotecan and AZD0156, that were tested. Irinotecan is a topoisomerase-I inhibitor and AZD0156 is an oral inhibitor of ATM kinase. To determine the *in vivo* pharmacokinetics, free plasma concentrations of Irinotecan and AZD0156 were measured in mice with LC-mass spectrometry for a period of 24 h. Based on these concentrations a dosing scheme for *in vitro* applications was developed. Petreus et al observed differences in response to the treatment between the 2D setup and the 3D setup that they introduced. Moreover, they were able to demonstrate similar treatment effects in the tumour spheroids of their 3D setup compared to *in vivo* mice studies. Just as for the design by Guerrero et al, the disadvantage of this system is the lack of parallelization [23]

Lastly, Schuster et al developed a system that consists of two separate devices, a 3D culture chamber platform that accommodates tumour organoids and a multiplexer device that delivers anti-cancer drugs and cell culture medium to the 3D culture chamber platform. Both devices are shown in figure 5.

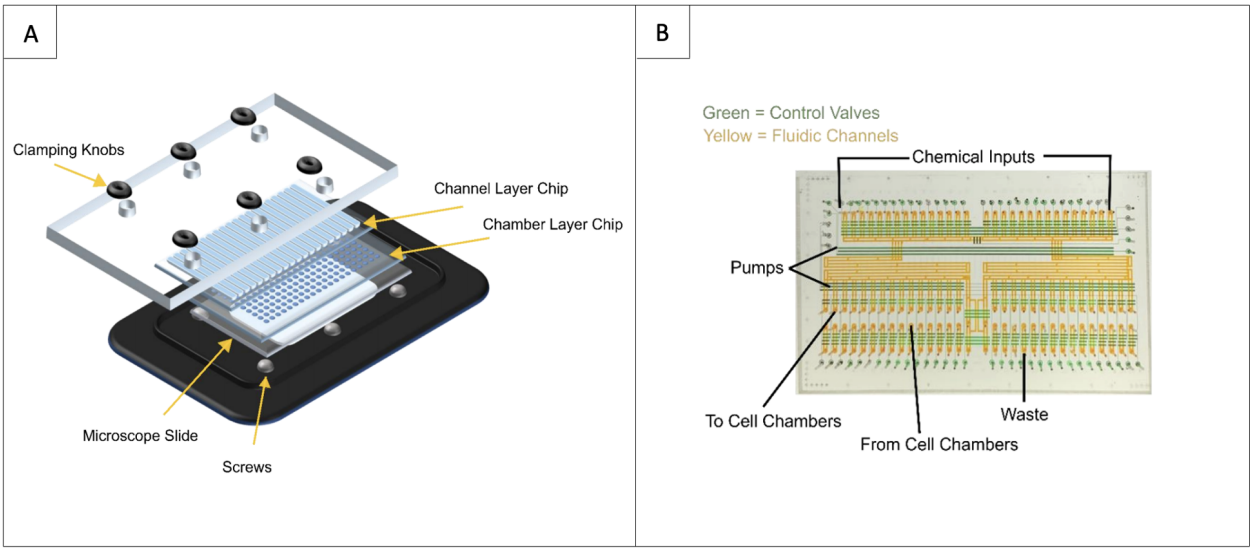

Figure 5: The designs of the A) 3D culture chamber platform and the B) multiplexer control device, developed by Schuster et al. Adapted from the supplementary figures [21].

The 3D culture chamber platform consists of 20 parallel channels, where each channel contains ten 3D culturing chambers. In the culturing chambers tumour organoids, derived from human pancreatic tumour tissue are placed. The multiplexer device is able to sequentially deliver different types of drugs and medium to the culture chambers, making it possible to deliver combinatory drug treatment and to deliver drugs for different periods of time. With custom-made software that controls the valves that are present in the multiplexer device, different combinations of drugs can be sequentially delivered to the channels of the 3D culture chamber platform. This system allows for high-throughput (200 organoids), combinatorial and temporal drug testing [21]. However, it was not shown that with this system it is possible to simulate the *in vivo* concentration profiles of the anti-cancer drugs that were tested, to such a degree as was achieved by Petreus et al. In addition, the system is quite complex and difficult to use in practice for drug testing experiments, due to the high amount of organoids that need to be integrated in separate chambers and the amount of tubing needed to connect in- and outlets.

1.4.2 TOP platform

In collaboration with academic and industrial partners, BIOS Lab-on-a-chip group and the Applied Stem Cell Technologies (AST) group developed the Translational Organ-on-Chip Platform, abbreviated by TOP. The idea of the TOP platform is to provide biologists with a universal platform on which different chip designs can be brought together, depending on the users' needs [29]. The system that was developed throughout this research needed to be able to be integrated in the TOP platform.

The platform consists of one general fluidic circuit board (FCB), shown in figure 6A, on which up to three different microfluidic building blocks (MFBBs), shown in figures 6B and 7, can be placed in a parallel manner [30].

Fluidic circuit board
The FCB consists of a total of 39 so called 'control channels', indicated by the green channels in figure 6A, that originate from 13 different inlets, situated at the right top corner in figure 6A. The 13 channels coming from these inlets all bifurcate into three channels, each leading to a different MFBB. The channels can either

be pressurized or depressurized. In this way, they act as an on/off-switch for the pneumatic valves that are integrated in the 64-chamber cell culturing MFBB. If pressure is applied in one of the control channels, the valves that are present along the path of this channel are closed. If atmospheric pressure is present in the channel, and no pressure is applied, the valves along its path are open. Moreover, the individual MFBBs can be switched 'ON' and 'OFF' by the three yellow channels. Each of the yellow control channels is connected to all 13 green control channels of a different MFBB and can close those if a pressure is applied to it. [30]

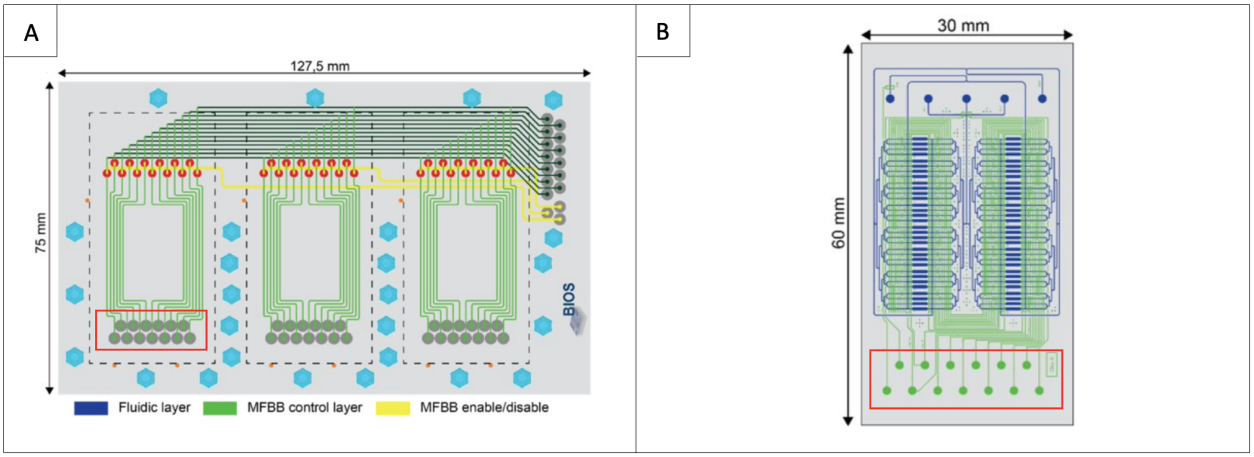

Figure 6: Schematic overview of the A) FCB design and the B) 64-chamber cell culturing MFBB. Reprinted from [31].

Microfluidic building blocks

Different MFBB designs, shown in figure 7, have been introduced for various applications, such as an organ-on-chip MFBB, a metering and mixing MFBB, a 64-chamber cell culturing MFBB and a droplet encapsulation MFBB [31]. Different configurations of MFBBs can thus be composed and new designs of MFBB can be developed for various purposes. The 64-chamber cell culturing MFBB, shown in more detail in figure 6B, is most interesting for the purposes of this project as it takes full advantage of the architecture of the FCB for control of the pneumatic valves on the MFBB. The control channels of the MFBB can be connected to the control channels on the FCB through the 13 outlets, indicated by the red box in figure 6A and the control channel inlets of the MFBB, indicated by the red box in figure 6B. Along the control channels on the MFBB there are multiple valves present that can close the fluid channels, shown as the blue channels in figure 6B. The fluid channels have 3 separate inlets that can be individually addressed with use of the control channels and valves. These inlet channels ultimately lead to 64 cell culture chambers. With use of the control channels, it can be set which chambers one wishes to access during measurements. [30]

The FCB makes it possible to control the valves of multiple MFBBs simultaneously. This way, MFBB operation can be automated and the addition of a second and third MFBB on the FCB does not require any additional pressure tubing to control the pneumatic valves, compared to using only one MFBB. Moreover, different combinations of MFBBs with different functions can be integrated on the FCB, making the system suitable for a wide range of applications.

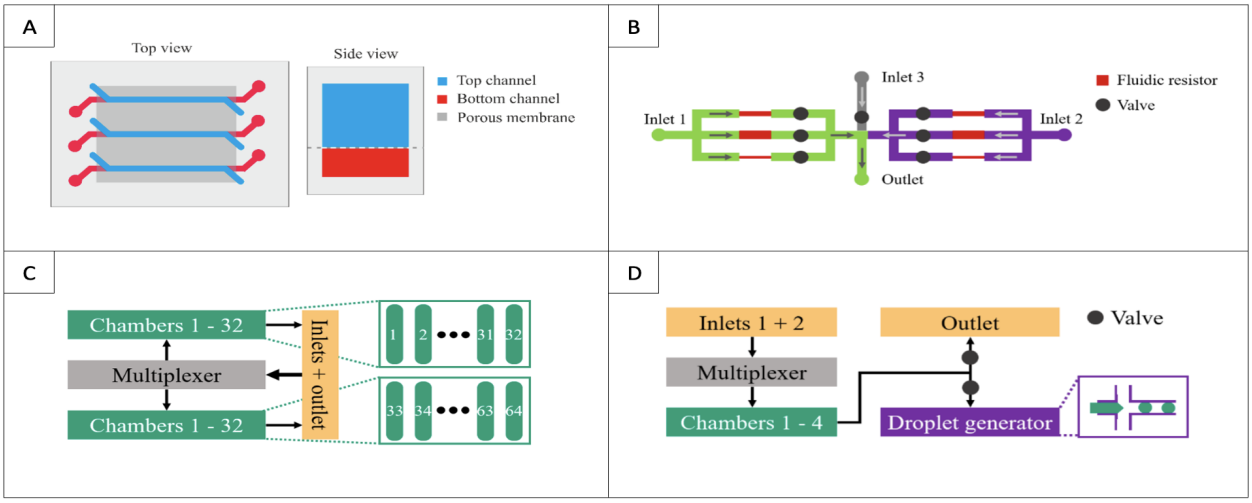

Figure 7: Schematic overview of the A) 3-organ-on-chip MFBB, B) Metering and mixing MFBB, C) 64-chamber cell culturing MFBB and D) Droplet encapsulation MFBB. Reprinted from [32].

Pneumatic valve working

The pneumatic valves that were used in the 64-chamber cell culturing MFBB and in the microfluidic chips designed throughout this project can be closed and opened by applying or releasing a closing pressure on the control channels leading to the valves. The valve consists of several layers, as indicated in figure 8. A PDMS layer (black) with the imprinted control channel is placed on another PDMS layer that was casted on a glass slide (dark blue). The top part of the control layer is extremely thin and acts as a membrane that is impermeable to liquid but permeable to gas. If pressure is applied on the control layer, the membrane is pushed into the flow layer (light blue), thereby closing off the control channel. The control channel cross-section is half rounded, such that the membrane can make contact with the entire channel, thereby closing off the channel. With a rectangular cross-section it would not be possible for the pneumatic valve to fully block the flow in the flow layer.

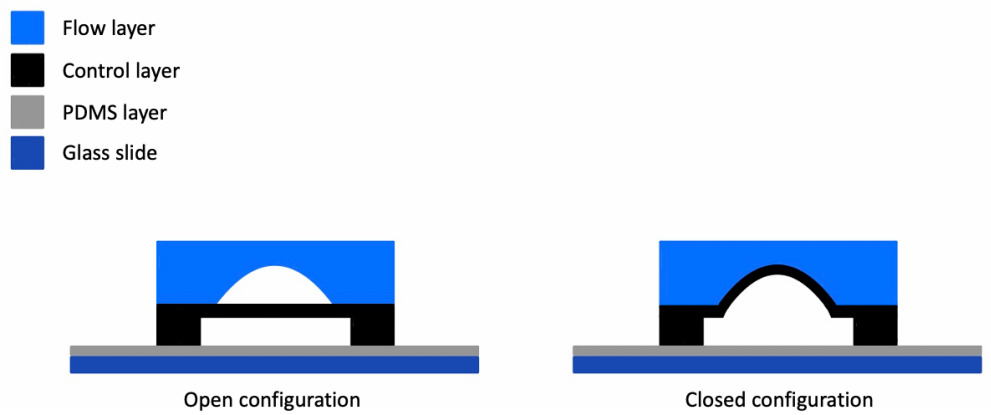

Figure 8: Schematic, cross sectional overview of the pneumatic vale in 'open' and 'closed' configuration. Adapted from [33].

1.4.3 Remaining problem

As discussed, different systems have been developed that can apply dynamic drug concentration profiles in a microfluidic system, by using different approaches. However, these systems are not parallelized to a degree that is sufficient to potentially replace currently used *in vitro* and *in vivo* mouse models. The TOP platform

has the potential to achieve further parallelization, while maintaining the ability to administer dynamic drug concentrations, but this has not been done yet.

2 Goal and requirements

The goal of this project is to design, fabricate and test a microfluidic system, with which different dynamic anti-cancer drug concentration profiles can be generated and supplied to multiple, parallel, microfluidic channels. This system should make use of the pneumatic valves, designed by BIOS Lab-on-a-chip group and should be implementable on the TOP platform.

2.1 Subgoals

The main goal can be divided into a total of five subgoals.

Subgoal 1 *Develop a microfluidic chip design for parallelization of flow over three microfluidic channels, making use of TOP compatible, pneumatic valves. The Drug Distribution Chip (DDC).*

Subgoal 2 *Develop a microfluidic chip design, that can be integrated on the TOP platform, for generating dynamic drug concentration profiles on chip, making use of TOP compatible, pneumatic valves. The Dynamic Concentration Generating Chip (DCGC).*

Subgoal 3 *Combine the DDC and DCGC in one system, to generate and sequentially supply different dynamic drug concentration profiles to multiple parallel channels with use of TOP compatible pneumatic valves.*

Subgoal 4 *Investigate the effect of in vivo anti-cancer drug concentration profiles on tumour spheroids in a parallel manner, with the developed microfluidic chips.*

Subgoal 5 *Integrate the developed microfluidic chips on the TOP platform.*

2.2 Requirements

2.2.1 Requirements for parallelization

- **Equal volume distribution** An equal volume should flow through all channels per time interval and over the entire period, with a maximum mutual difference in volume of 10%.
- **Stable flow rate** The amount and magnitude of perturbations in the flow rate over time should be minimized. The flow rate in all channels should stay within a range of 50% standard deviation of the target flow rate (6 - 10 µL/min). Furthermore, the flow rate should never drop beneath 0 µL/min or exceed 20 µL/min.
- **Overcoming disturbances** Above requirements should also be met if differences in hydraulic resistance between channels arise due to air bubbles or other obstacles that might be introduced in the channels during experiments.
- **Sequential parallelization** Intermittent parallel flow is allowed if the volume, after which a switch between channels is initiated, is such that the volume above the spheroid culture well is refreshed, for optimal supply of oxygen and nutrients. The set flow rate should be sequentially supplied to all channels. After the desired volume is injected in one channel, the flow switches to the second channel, where the same volume is injected. Subsequently, the flow switches to the next channel. This loop should then be repeated for the duration of the experiment.

2.2.2 Requirements for generation of dynamic drug concentration profiles

- **Multiple profiles** The system should be able to generate multiple dynamic drug concentration profiles of different anti-cancer drugs
- **High dynamic range** The drug concentration can take values within a 1000x range of e.g. 20 nM – 20 µM.
- **Four concentration steps** At least four steps in drug concentrations can be realized that cover the lowest and highest concentration of a specific concentration profile.

- **Low half-life time** A 50% reduction in drug concentration can be realized within 10 minutes.

2.2.3 Drug distribution chip (DDC) and dynamic concentrations generating chip (DCGC) requirements

- **TOP integration** The chips can be integrated on the TOP platform. Therefore, the design should comply with the ISO standards [34].
- **Proper valve closing** The pneumatic valves on the chips should be able to fully close of a channel and block all the flow through the channel.
- **Software control** The system should be easily controlled through software to open and close the pneumatic valves at specific times and generate the desired drug concentration profiles.
- **Prevention of backflow** A fluid flow should only be present in the channel that is open and there should be no backflow from the open channel into one of the other channels that are closed.
- The DDC should comply with the parallelization system requirements (see 2.2.1) and the DCGC should comply with the dynamic drug concentration profile generating system requirements (see 2.2.2).

3 Materials and methods

3.1 Microfluidic chip fabrication

3.1.1 Drug Distribution Chip (DDC) and Dynamic Concentration Generating Chip (DCGC) fabrication

The same chip design was used for both the DDC and DCGC. Four reservoirs can be connected to the DCGC to generate a dynamic concentration profile. The DDC is placed in a mirrored manner to the DCGC, where one flow can be sequentially distributed over four channels. Moulds for the DDC and DCGC were prepared with the micromilling machine in the rapid prototyping lab at the BIOS Lab-on-a-Chip group. Micromilling is a microfluidic chip fabrication technique, with which microscale features can be created by cutting away bulk material [35]. Two moulds were produced, one for the flow layer, with the negative flow channels and one for the control layer, with the negative control channels. A 7 mm thick, 7 x 5 cm block of PMMA was placed in the micromilling machine. The CAD file, created in SolidWorks, with the desired features for the flow layer or the control layer, was loaded onto the machine.

The DDC and DCGC were prepared using replication moulding. The microfluidic chips consist of multiple layers, where for each layer the fabrication process differs. The flow layer was produced by pouring a 7:1 w/w mixture (8 g) of special RTV 615 PDMS and curing agent on the mould for the flow layer. Subsequently, the control layer was produced by pouring a 20:1 w/w mixture (3.15 g) of RTV 615 PDMS and curing agent on the mould for the control layer, which was then spin coated at 200 rpm for 60 s, resulting in a 30 µm thick membrane at the valve site. Both moulds were placed in the oven for 30 min at 60 °C for pre-curing. Subsequently, 1 mm inlets were punched in the flow channels, after which the flow layer and control layer were aligned and bonded together. To further cure and bond the two layers, the chip was placed in the oven for 45 min at 60 °C. In the mean time, a base layer of 10:1 w/w PDMS and Sylgard 184 curing agent (Dow Corning, US) was spin coated on a 1 mm thick, 75 x 38 mm glass slide (Corning, US) at 300 rpm for 60 s, after which it is placed in the oven for 20 min at 60 °C. After the waiting time, both parts are taken out of the oven and 0.75 mm inlets were punched in the control layer channels. Lastly, the control layer was bonded to the PDMS layer on glass. After bonding, the chip is placed in the oven at 60 °C overnight to fully cure and bond all layers.

The design of the DCGC and DDC is shown in figure 9A. The chip consists of one inlet channel, that bifurcates into four channels. Each channel can be independently opened and closed by the pneumatic valves. The channels are 2 mm in width, 500 µm in height and the length from the inlet to the outlet of one of the four channels is approximately 35 mm. The channels are rectangular in form from inlet to the second bifurcation, but are half rounded in form after the second bifurcation, over the length were the pneumatic valves are situated. This form is needed to fully close the channels, as was discussed in section 1.4.

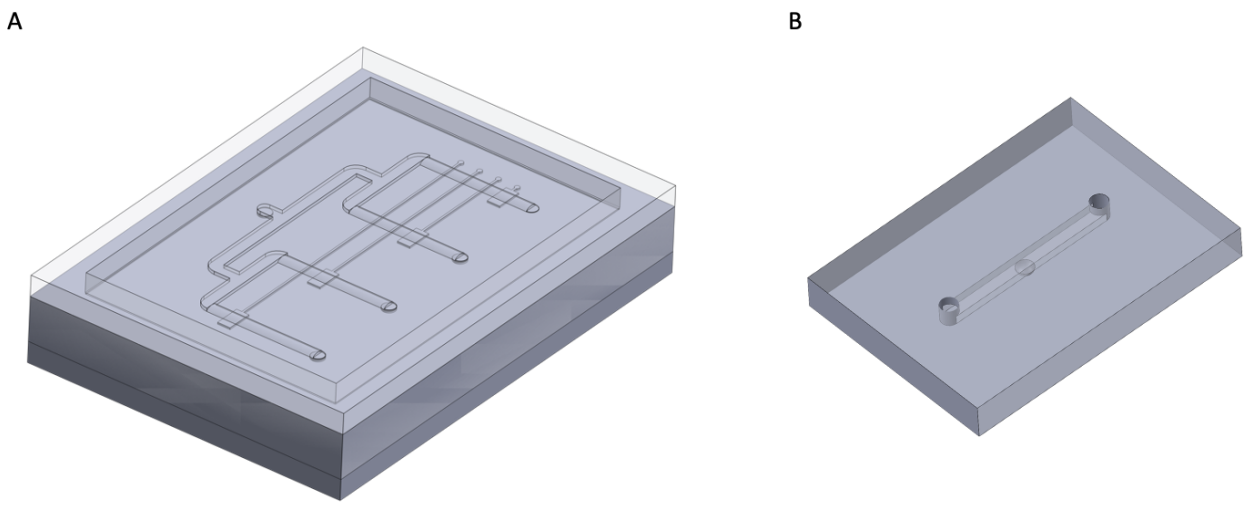

Figure 9: Designs of the A) DCGC and DDC and the B) TSoC, used in the final system. The designs were produced in SolidWorks.

3.1.2 Tumour-Spheroid-on-Chip (TSoC) fabrication

Moulds for the Tumour-Spheroid-on-Chip (TSoC) were prepared by micromilling. The TSoC consists of two parts, one bottom part with a well to accomodate a tumour spheroid and a top part with flow channel. For both parts of the chip a separate mould was produced by micromilling.

The top and bottom parts of the TSoC were prepared using replication moulding. A 10:1 mixture of PDMS and a curing agent was poured on the moulds to imprint the features in the PDMS. A total of 35 g PDMS and curing agent was needed in order to produce 12 top parts and 18 g PDMS and curing agent to produce 9 bottom parts. Subsequently, the moulds were placed in the oven at 60 °C overnight. The next day, 1 mm in- and outlets were punctured in the channels of the top parts. ARcare 8938 adhesive tape (Adhesives Research, US) was used to bond top and bottom parts together. The channel cutout was made with a Cricut machine (Cricut, US).

The design of the TSoC is shown in figure 9B. The TSoC has a rectangular channel of 2 mm in width, 1 mm in height and 21 mm in length. The culture well has a diameter of 2 mm and a volume of 2 µL.

3.2 Cell culturing

3.2.1 HCT-116

Human colon cancer cells (HCT-116) were cultured in McCoy's 5A medium with glutamine, supplemented with 5% Fetal Bovine Serum (FBS) and 1% penicillin streptomycin (pen/strep) in T-25 cell culture flasks. The cells were stored in an incubator at 37 °C and 5% CO_2 and passaged every three days into fresh medium, up to a maximum passage number of 30. Passaging was performed when cell confluency reached 80 %. First, the cell culture medium was removed and cells were washed with 5 mL PBS. Then, 2 mL trypsin was added and the cell culture flask was placed in the incubator for 5 min at 37 °C for the cells to fully detach from the surface. Subsequently, 8 mL of McCoy's 5A medium was added to the cells and trypsin and the total volume of 10 mL was centrifuged at 390g for five min in a 10 mL tube. The pellet of cells at the bottom of the tube were resuspended with 2 mL of cell culture medium and split 1:5 or 1:10, depending on the period between the current and the next cell passage.

3.2.2 Tumour spheroids

HCT-116 cells were diluted in McCoy 5A medium to reach a concentration of 10.000 cells per milliliter. For the preparation of one spheroid, 200 µL was pipetted in a well of a Nunclon Sphera 96-well U-bottom plate,

achieving a seeding density of 2.000 cells per well. The plate was then centrifuged at 390g for five min, to create a cluster of cells in the well. The wells were imaged after centrifugation to check for an equal amount of cells per well. After four days of culture, the spheroids were imaged for roundness, density and size. At a seeding density of 2.000 cells per well, the spheroids are approximately 500 µm in diameter.

3.3 Software

The software with which the system, developed throughout this project (4.1), can be controlled is produced by Convergence. Convergence is a company based in Enschede, the Netherlands, focused on designing and manufacturing customized fluid handling systems [36]. The Convergence software uses LabVIEW (NationaL Instruments) as a main driver and provides an intuitive user interface [37]. An overview of the user interface is shown in figure 33 in appendix A.

In collaboration with Felix Broens, from Convergence, a program was developed to automate experiments with the system. The program consists of different layers, where each layer has its own sub-program. The scripts of these (sub-)programs can be found in appendix A. The main program contains instructions for setting a specific flow rate, logging data, opening and closing valves to get the starting configuration of valves and for running the sub-programs. One sub-program, the parallelization protocol, contains the instructions for the parallelization loop and is looped throughout the total duration of the set experiment time. It opens the valves in a sequential manner and is programmed such that switching of channels occurs after a certain volume has passed the channel. Other sub-programs contain contain the information for switching between the four reservoirs. An overview of how the automation program works is shown in appendix A, figure 34.

The flow rate is controlled by a proportional integral derivative (PID) controller. A schematic overview of how this controller works is shown in figure 10. The PID controller measures the flow rate being present and compares it to the set point. Based on the difference between measured flow rate and set point, the controller either increases or decreases the pressure that is applied to the reservoir, depending on the measured value being lower or higher than the set point. This relation is represented by formula 1, where the error is given by the difference in set point (SP) and process variable (PV).

$$e(t) = SP - PV \tag{1}$$

The PID controller output ($u(t)$) is given by formula 2, where PG is the proportional gain, T_I the integral time in seconds and T_D is the derivative time in seconds. The output ($u(t)$) of the PID controller is processed into the value PV, which is then compared to the SP to determine the input error ($e(t)$) for the PID controller. In this way, a stable flow rate is realized at the desired value.

$$u(t) = PG\left[e(t) + \frac{1}{T_I}\int_0^t e(t)dt + T_D\frac{de(t)}{dt}\right] \tag{2}$$

The PG sets the magnitude of the proportional term as its value is multiplied with the measured error between SP and PV. The integral term integrates over the past values of e(t) and grows with time if the error persists. The value T_I determines the magnitude of the integral term, where the integral term is inversely proportional to T_I. The derivative term estimates the future value of e(t) based on its measured rate of change and can give a dampening effect. However, it is sensitive to rapid changes in the measured value. Therefore it is not used in the flow rate control loop in our system, as sharp peaks in flow rate can occur when switching channels during parallelization and this would lead to an unstable flow rate profile. [38]

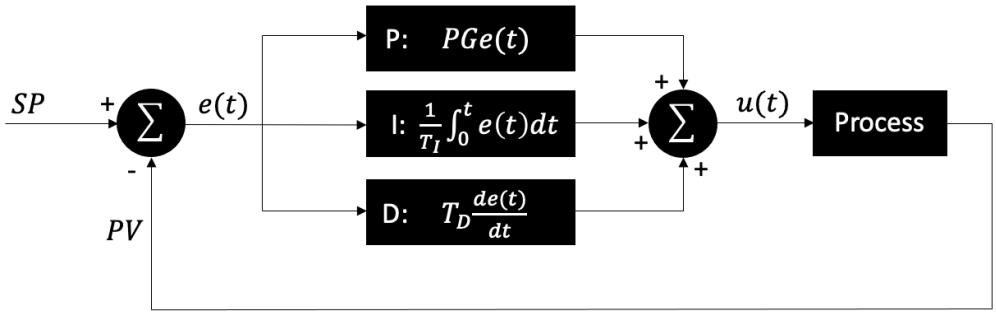

Figure 10: Schematic representation of the PID controller feedback loop.

3.4 Experimental procedure for parallelization experiments

3.4.1 Parallelization with rotary valves

To examine whether flow can be steadily parallelized, a flow was sequentially parallelized over three TSoCs using commercially available equipment from Fluigent. This gives insights into the characteristics of the system and it provides the possibility to investigate whether sequential parallelization is a suitable solution for maintaining steady, identical flow rates in all channels, before moving on to actually developing microfluidic chips.

The setup used for this experiment is shown in figure 14 in the results section (4.2.2). The specific tubing that was used in this setup is shown in figure 35 in appendix B.1. A 100 mL glass reservoir (Sigma-Aldrich, US) was filled with 20 mL DI water and connected to outlet 3 of the MFCS-EX pressure controller (Fluigent, France) with pressure tubing. The reservoir is connected to a M flow sensor (Fluigent) with liquid tubing. The M sensor was then connected to the central inlet of the M-switch rotary valve (Fluigent) and outlets 1,2 and 3 of the M switch were connected to TSoCs. Finally, the outlets of the TSoCs were led to separate 50 mL waste vials. In the Automation Tool software (Fluigent), a protocol was created, to set a flow rate of 6 µL/min and a volume injection of 2 µL per interval per channel, with the function 'flow rate, volume injection'. In this way, the flow is switched between channels 1,2 and 3 after a volume of 2 µL has passed and the flow is sequentially parallelized. This loop needs to be repeated 2880 times, such that the experiment runs for a total of 48 h. The captured volumes in each capture vial was determined by weighing each vial. The average flow rate per channel was determined based on the volume per capture vial and the duration of the experiment.

The experiment was repeated with cell culture medium instead of DI water, for a duration of 96 h. For this experiment, the 100 mL glass reservoir was filled with 40 mL McCoy's cell culture medium.

3.4.2 Parallelization with microfluidic chips

The approach for steady parallelization of flow, with microfluidic chips, was tested in the same manner as discussed in section 3.4.1. By substitution of the M-switch rotary valve with the DDC, the system can take full advantage of the functions that the TOP platform offers, such as automated and simultaneous operation of multiple MFBBs without the need for additional pressure tubing and plug and play with other types of MFBBs.

The setup used for this experiment is shown in figure 20 in the results section (4.2.5), and consists of exactly the same components as the setup described in section 3.4.1, where only the M-switch rotary valve was replaced by the DDC and the Convergence Inspector Hydra (Convergence, Netherlands) was added, to be able to control the pneumatic valves of the DDC. The specific tubing that was used in this setup is shown in figure 36 in appendix B.2. When setting up the system, the pressure lines of the pneumatic valves were first filled with DI water and connected to the pneumatic valve inlets of the DDC. The closing pressure of the valves was set at 1.5 bar.

In the Convergence Inspector software interface, the flow rate was set at 10 µL/min and the volume injection per interval per channel was set at 3.5 µL. The experiment duration was 72 h. The average flow rate per channel was determined based on the volume per capture vial and the duration of the experiment.

3.5 Experimental procedure for generating dynamic concentration profiles

In order to generate dynamic concentration profiles, four reservoirs were connected to different ports of a rotary valve. With the rotary valve, it is possible to set from which reservoir fluid is tapped. In this way, it is possible to cover a maximum of ten different concentration steps of a certain drug concentration profile. The ability of this method to generate dynamic concentration profiles on chip was investigated with fluorescein. The setup that was used for the experiment is schematically shown in figure 22. The specific tubing that was used in this setup is shown in figure 37 in appendix B.3. A total of four 15 mL p-cap reservoirs (Fluigent) were filled with different concentrations (10, 5, 1 and 0 µM) of fluorescein sodium salt (molecular weight, 332 Da, Sigma-Aldrich) in DI water. The reservoirs were connected to outlet 3 of the MFCS-EX pressure controller pressure tubing that is split into four, using air splitters. The reservoirs were each connected to different ports on the M-switch rotary valve. The outlet of the M-switch was connected to the inlet of a M flow sensor and the outlet of the M sensor was then connected to one TSoC. The outlet of the TSoC was led to a 10 mL capture tube. In the OxyGEN software (Fluigent) interface, a protocol was created to sequentially tap from reservoir one (10 µM fluorescein) to four (DI water), with 30 min time periods at a flow rate of 10 µL/min. The experiment duration was 180 min, in order to capture all the concentration steps. The microfluidic channel of the TSoC was imaged with an EVOS microscope (ThermoFisher, US). Fluorescence images of a specific part of the microfluidic TSoC channel were taken at an one minute interval, using a GFP (green fluorescent protein) filter. Analysis of the images for fluorescence intensity was performed in ImageJ [39]. The measured fluorescence intensity was corrected for background signal.

3.6 Experimental procedure for parallelization of dynamic concentration profiles

The experiments discussed here are performed with the system designed throughout this project, which is schematically shown in figure 11. The specific tubing that was used for this system is shown in figure 38 in appendix B.4. When setting up the system, the pressure lines of the pneumatic valves were first filled with DI water and connected to the pneumatic valve inlets of both the DCGC and DDC, according to numbering shown in figure 11. Four 15 mL p-cap reservoirs are connected to the inlets on the DCGC. The reservoirs were connected to outlet 3 of the MFCS-EX pressure controller with pressure tubing, that was split into four, using air splitters. The outlet of the DCGC was connected to the inlet of the M sensor and the outlet of the M sensor was then connected to the DDC. Three of the four outlets of the DDC are connected to a TSoC, where the fourth outlet is used as a waste channel. The outlets of the TSoCs are connected to separate capture tubes. The pneumatic valves, indicated in red, of both the DCGC and the DDC are connected to the Convergence Inspector Hydra, with which a closing pressure (1.5 bar) was applied to individual valves.

3.6.1 Validation experiment with fluorescein

The ability of the system to generate dynamic drug concentration profiles and supply them to multiple TSoCs was investigated with fluorescein. In this experiment, 60 cm 1/32" ID Teflon tubing was used between the M sensor and the DDC, to be able to image the TSoC under the microscope. Four 15 mL p-cap reservoirs were filled fluorescein concentrations of 10, 5, 1 and 0 µM, with a volume of 10 mL per reservoir. The four concentration steps of fluorescein, with periods of 30 min per step, were parallelized over three TSoCs at a flow rate of 10 µL/min. Switching of channels in the DDC occurred after a cumulative volume of 3.5 µL had passed. The four 30 min concentration steps were repeated throughout the total duration of the experiment (1000 min). The microfluidic channel of one TSoC (chip 1) was imaged with a fluorescence microscope. Images were taken again at a 1 min interval with a fluorescence microscope (Leica DM IRM, Germany) and processed as described in section 3.5. The outlets of all three TSoCs were connected to separate waste vials. The waste in each waste vial was analysed for fluorescence intensity, to determine whether the concentration steps were properly parallelized. To do this, 200 µL of the waste of each TSoC was pipetted into separate

wells of a 96-well plate. To be able to compare the intensity measured, 200 µL of the four concentration steps was also pipetted into separate wells of the 96-well plate. Lastly, the volume of the waste was measured to verify equal distribution of volume over time.

3.6.2 Investigating spheroid growth on parallel TSoCs

To examine whether the tumour spheroids can survive and grow on the system during sequential parallelization, three TSoCs were exposed to cell culture medium for a period of 48 h.

Four days in advance to the experiment, the spheroids, DDC and DCGC, and top-, bottom- and adherent tape parts for the TSoC were prepared according to protocol 3.2.2, 3.1.1 and 3.1.2, respectively.

One day in advance to the experiment, 60 mL of McCoy's 5A cell culture medium was placed in the incubator in a T-75 cell culture flask (ThermoFisher) for degassing of the medium.

At the day of the experiment, spheroids were first checked for roundness, density and size. The DDC and DCGC were plasma treated in a CUTE plasma oven (Femto Science, Germany) for sterilization and placed in a sealed petri dish. Before setting up the system in the lab, the TSoCs were coated with pluronic F-127 (Sigma-Aldrich) to prevent spheroids from adhering to the well. The bottom parts of the TSoC were first placed on the humidity box insert, where the adhesive tape was placed on the bottom parts. In each well, 8 µL of pluronic F-127 was pipetted, after which a cover of PDMS was placed over the well to prevent them from drying. Then, the humidity box was closed and placed in the incubator for 2 h. Meanwhile, the system was set up in the lab. The four p-cap reservoirs were filled with 10 mL of McCoy's 5A cell culture medium. After 2h, the spheroids were seeded into the wells. First, the pluronic F-127 was removed and the wells were washed with 2 µL of cell culture medium. Then, 2 µL of cell culture medium was again pipetted into the wells. With a wide bore pipette tip (ThermoFisher) fluid from one well of the Nunclon Sphera 96-well U-bottom plate was pipetted into the tip at 50 µL, to obtain the spheroid. After sinking of the spheroid to the bottom of the pipet tip, the tip was brought into contact with the well to release and place the spheroid. Afterwards, the top parts of the TSoCs were placed and the TSoCs could be connected to the system. The TSoCs were attached to the outlets of the DDC one by one at a flow rate of 20 µL/min. Placement of the tubing into the in- and outlets had to be gentle, to prevent flushing out the spheroids from the well.

The flow rate was set at 10 µL/min and the cumulative volume after which a switch in channels is initiated during parallelization was set at 3.5 µL. Cell culture medium was sequentially tapped from each reservoir, for periods of 750 min.

The surface areas of the spheroids at t = 0 h and t = 48 h were converted into volumes in ImageJ, which were then used to determine the growth in volume over time. The growth of the spheroids was plotted as percentual growth of initial volume.

3.6.3 Parallelization of the dynamic *in vivo* Oxaliplatin concentration profile

To validate the system as an adequate *in vitro* model for parallel anti-cancer drug testing, the *in vivo* concentration profile of oxaliplatin was parallelized over three TSoCs. The TSoCs used in this experiment consisted of three wells, placed in series. In this way, nine colorectal tumour spheroids could be exposed to the *in vivo* oxaliplatin concentration profile. A fourth TSoC was exposed to cell culture medium for the duration of the experiment to function as a control.

The steps for preparation of the experiment, setting up the system and the seeding of spheroids on chip were described in section 3.6.2. For this experiment, the four reservoirs were filled with oxaliplatin concentrations of 9, 3, 1 and 0.5 µM, with volumes of 3, 3, 10 and 15 mL, respectively. The time periods for the concentration steps were set at 15, 105, 960 and 1800 min, respectively. The flow rate was set at 6 µL/min and the cumulative volume after which a switch in channels is initiated during parallelization was set at 2 µL.

The control was set up separate from the parallelization experiment. A 100 mL glass reservoir was filled

with 10 mL McCoy's cell culture medium and connected to outlet 4 of the MFCS-EX pressure controller with 1.5 m Tygon R-3603 6 mm OD, 4 mm ID pressure tubing that was connected to a piece of 40 cm Masterflex 335L 4 mm OD, 1.6 mm ID pressure tubing. The reservoir was connected to a L flow sensor (Fluigent) with 30 cm 1/32" ID Teflon tubing. The outlet of the flow sensor was connected to the inlet of the TSoC with 30 cm 1/25" ID Tygon tubing. A piece of 30 cm 1/25" ID Tygon tubing was used as outlet tubing and connected to a 50 mL waste vial. In the OxyGEN software, the flow rate was set at 2 µL/min for a period of 48 h.

The surface areas of the spheroids at t = 0 h and t = 48 h were determined in ImageJ. The areas were converted into volumes, which were then used to determine the growth in volume over time. The growth of the oxaliplatin treated spheroids were compared to the growth of the control and plotted as a percentual growth to control. This was done for each individual TSoC, by taking the average growth of the three spheroids that were placed in series.

4 Results and discussion

4.1 System design for parallelization of dynamic drug concentration profiles

A schematic overview and photos of the system, designed throughout this project, are shown in figure 11 and 12, respectively. With the system, it is possible to supply up to four different concentration steps to three different microfluidic channels and one waste channel. To the three microfluidic channels, TSoCs can be connected, in which tumour spheroids can be seeded. Therefore, experiments can be performed in triplicate. Pressure can be be applied on the liquid in the 15 mL reservoirs by a pressure controller. Each reservoir is connected to a different inlet on the DCGC, such that different concentrations of anti-cancer drugs can be loaded in the reservoirs and can be delivered to the spheroids in a sequential manner, to cover the desired *in vivo* concentration profile. The DCGC is then coupled to the DDC, where in between a flow sensor is placed. With the flow sensor and the pressure controller, a feedback loop can be created, such that a certain flow rate can be set and maintained over time. Moreover, the cumulative volume that has flown through a channel can be monitored to initiate a switch between channels after the desired volume has passed. The TSoC chips are connected to the outlets of the DDC. The pneumatic valves, indicated in red, of both the DCGC and the DDC are connected to the Convergence Inspector Hydra, with which pressure can be applied to individual valves. With the DDC, the anti-cancer drug concentration profile can be sequentially parallelized over the three TSoCs, by opening the channels one after another for a certain period of time.

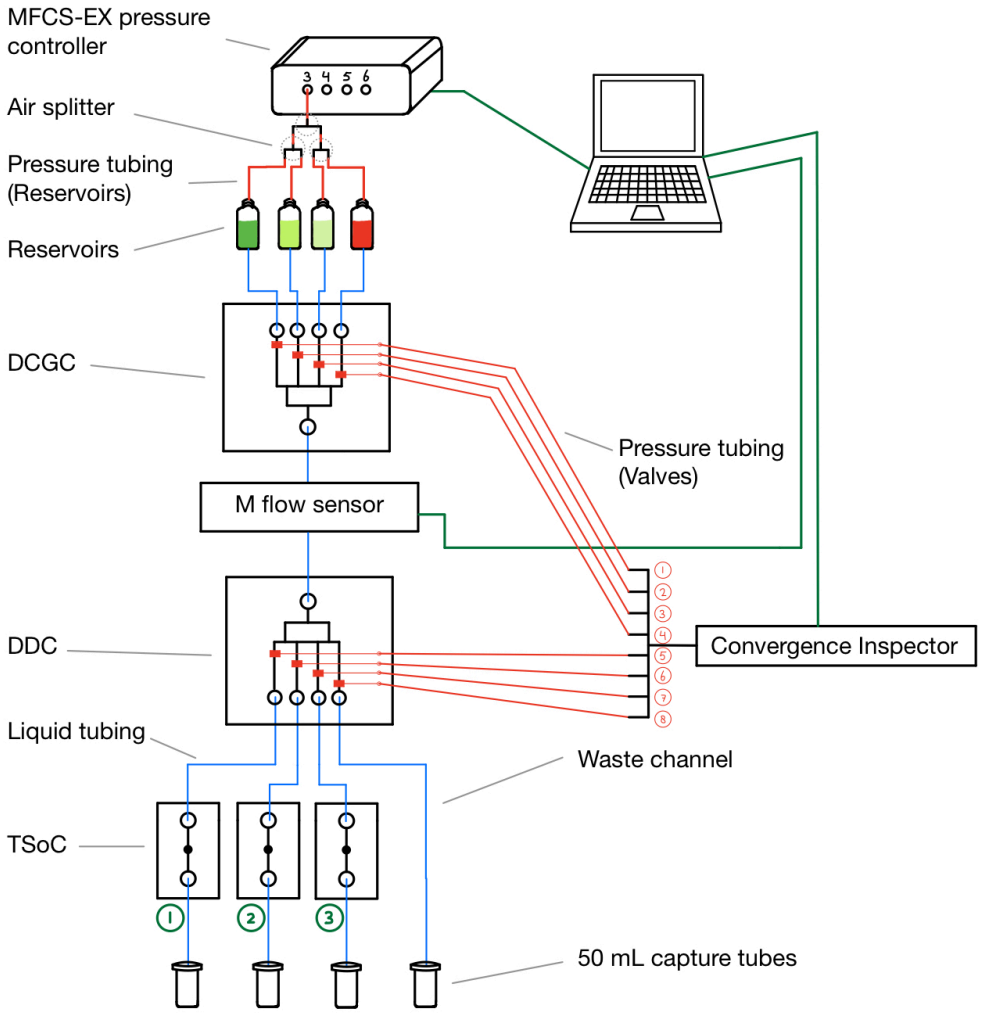

Figure 11: Schematic overview of the system designed throughout this project.

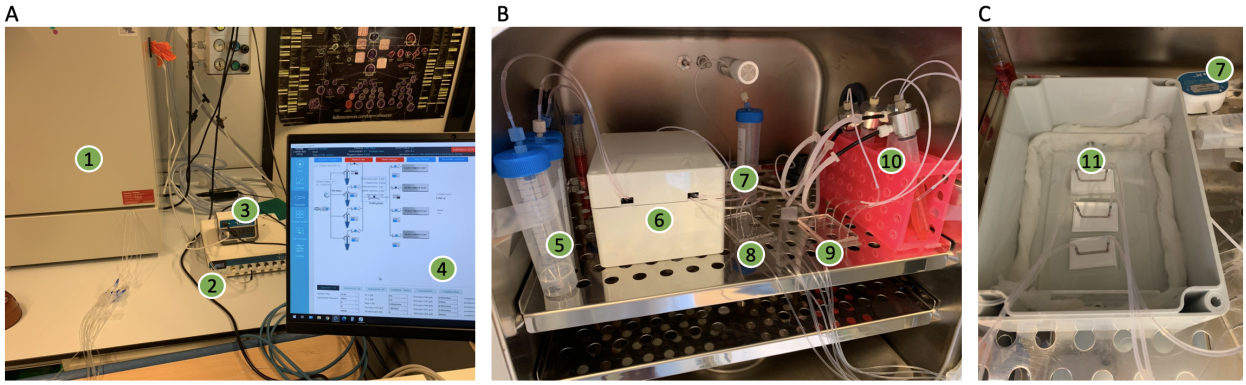

Figure 12: Photos of the system used in the lab. A) The setup outside of the incubator. B) The setup inside the incubator. C) The TSoCs inside the humidity box. (1) = Incubator, (2) = MFCS-EX pressure controller, (3) = Flowboard, (4) = Convergence Inspector software, (5) = Capture tubes (50 mL), (6) = Humidity box, (7) = M flow sensor, (8) = DDC, (9) = DCGC, (10) = P-cap reservoirs, (11) = TSoCs.

4.2 Sequential parallelization of flow

One of the main objective of this project was to steadily parallelize flow over multiple channels. Maintaining an identical flow rate over time in multiple, parallel channels simultaneously is difficult, as small differences in hydraulic resistance between channels already affect the equal distribution of flow over these channels. As identical conditions are required in each channel to be able to draw definite conclusions in future experiments, the decision was made to focus on sequential parallelization. During sequential parallelization, flow is applied to one channel for a certain period, after which the flow is switched to the next channel. This is looped throughout the duration of the experiment. In this way, each time that the flow is present in a channel of a TSoC, the volume above the well is refreshed, for optimal supply of oxygen and nutrients.

In this section, the ideal settings and equipment were first investigated for performing experiments with microfluidic chips. Thereafter, it was investigated whether flow could be steadily parallelized over three channels using commercially available equipment from Fluigent. With this equipment, which is readily available, an approach for steady, sequential parallelization could be developed and optimized before actually developing microfluidic chips ourselves. Finally, an approach was developed and tested to achieve steady, sequential parallelization with microfluidic chips, that can potentially be integrated on the TOP platform.

4.2.1 Effect of the type of flow sensor on the stability of the system

There are different types of commercial flow sensors on the market that can be used for measuring flow rates. Fluigent is a manufacturer of different fluid control systems in the field of microfluidics and fabricates several different types of flow sensors [40]. Their sensors range from a XS to a XL flow sensor. The flow sensors that are of interest for this project are the M and the L flow sensors, as they can measure flow rates in the range of 0 - 80 µL/min and 0 - 1 mL/min, respectively. Both sensors have different specifications. The M sensor has an ID of 430 µm and is connected to tubing with a 150 µm inner diameter. This significantly increases the hydraulic resistance of the system and thus increases the pressure that is needed to induce a certain flow. The higher pressure, placed on the reservoir, needed to induce flow can lead to air bubble formation [41]. In contrary to the M sensor, the L sensor has a 1 mm ID and can be directly connected to the 1/32" ID tubing. Even though potential problems with air bubble formation will likely not be an issue with the L sensor, the total hydraulic resistance of the entire system being low causes other problems. The low hydraulic resistance when using a L sensor results in no to little pressure being needed for fluid to flow through the system and therefore the pressure controller cannot properly control the flow rate. This is not a problem when using the M sensor due to the high resistance it introduces to the system. To circumvent this problem, 5 cm 100 µm ID tubing was connected at the outlets of the three TSoCs and waste channel when using the L sensor, thereby significantly increasing the hydraulic resistance of the system.

To investigate which sensor provides the most stable system, the setup as shown in figure 11 was used for sequential parallelization of DI water over three TSoCs. Either the M sensor or the L sensor was used between the DDC and DCGC to establish the flow rate control loop. At the outlets of TSoC 1 and 2 a flow sensor was connected to be able to measure the flow rate at the outlet. The resulting flow rate profiles when using the M or L sensor are shown in figure 13.

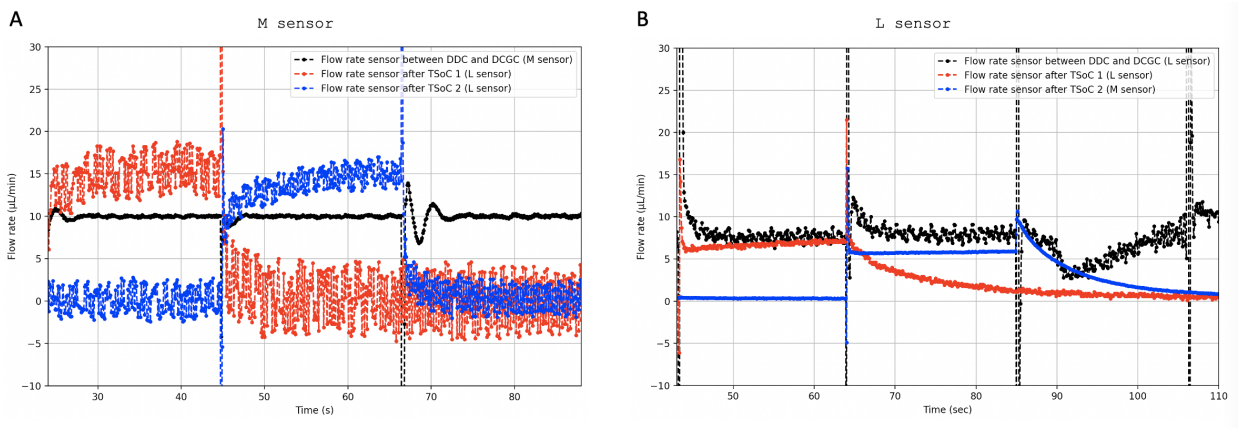

Figure 13: Flow rate profiles during sequential parallelization, using the A) M sensor or the B) L sensor to to establish a flow rate control loop. The black graph indicates the flow rate that is measured by either the M or L sensor that is placed before between DDC and DCGC. The red and blue graphs indicate the flow rate measured by the sensors that are placed after TSoC 1 and 2, respectively. Flow rates measured by the M sensor represent the true flow rate being present. In the period that is shown for both graphs, the flow was first applied to TSoC 1, then to TSoC 2 and lastly to TSoC 3. Switching times were t = 45 s and t = 67 for A) and t = 63 s, t = 85 s and t = 107 s for B).

It becomes apparent that the M sensor proved most stable in achieving a flow rate of 10 µL/min when comparing the black graphs of 'the flow rate sensor before chips'. The flow rate profile for the L sensor is noisy and more constant for the M sensor. The flow rate stays steadily around the value of 10 µL/min for the M sensor, whereas the L sensor shows a measured flow rate that was lower than the set flow rate. Moreover, the M sensor showed a much quicker recovery to a steady flow rate when disturbed, compared to the L sensor. When taking a look at the flow sensors that were placed after the chips, it becomes apparent that the flow profiles measured by the L sensor were again much more noisy. On top of that there seems to be a discrepancy in the measured flow rate between the L and M sensors, where the L sensor measures a flow rate with a factor 1.5 larger than what is measured by the M sensor. In characterization experiments it was determined that the M sensor measures the actual flow rate being present, indicating that the L sensor provides less accurate measurements. Based on these results it was decided to integrate the M sensor in the system.

4.2.2 Parallelization with rotary valves

In this experiment, flow was sequentially parallelized through three chips in the incubator. The setup used for this experiment is shown in figure 14. This was first done with DI water for a period of 48 h to investigate the stability of the system. Subsequently, the experiment was executed with cell culture medium for 96 h to investigate whether this system can potentially be used for longer periods and is compatible with cell culture medium, as future experiments with tumour spheroids will be performed. The flow rate was set at 6 µL/min and the volume after which the flow is switched between channels was set at 2 µL, such that each channel was subjected to a flow for approximately 20 s and static conditions for 40 s every minute. This cycle is then repeated throughout the total duration of the experiment, where one cycle is referred to as an iteration.

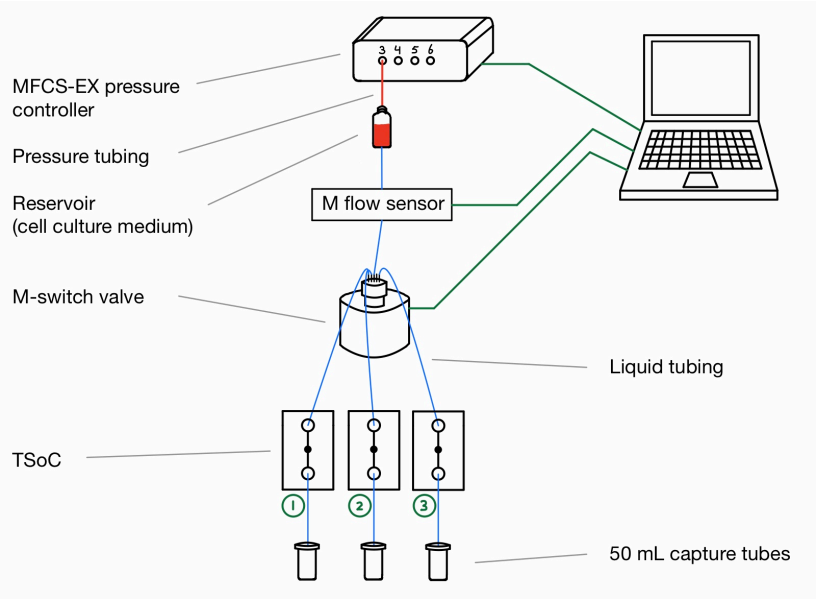

Figure 14: Schematic overview of the setup used for sequential parallelization with commercially available equipment.

The results for the experiment with DI water are shown in figure 15, where the average flow rate that was present throughout the experiment per chip is shown. The average flow rate per chip was based on the volume that has flown through each microfluidic chip and the total duration of the experiment. All values for the average flow rate per chip lie in close proximity of each other, with a difference of only 3.81 % between the highest and lowest value. The same percentual difference of 3.81 % was observed between the set flow rate and the biggest outlier (chip 3). Very similar results were obtained for the experiment with cell culture medium, as shown in figure 16. The difference in average flow rate between the highest and lowest value was only 4.21 %, with a percentual difference of 3.17 % between the set flow rate and the biggest outlier (chip 2). For both experiments, the requirement of equal volume distribution, where a maximum of 10 % difference in volume between channels was required, is met. The average flow rate ± standard deviation, determined over all the flow rate data points that were measured by the M flow sensor throughout the experiment, was 6.04 ± 2.94 µL/min for the experiment with DI water and 5.98 ± 2.92 µL/min for the experiment with cell culture medium. Thus, the measured flow rates are in good accordance with the set flow rates. Moreover, the standard deviation in measured flow rate was within the required range of 50 % standard deviation of the target flow rate. These results show that the flow sensor/pressure controller feedback loop functions properly and is able to maintain the same flow rate of 6 µL/min in all three chips throughout the experiment.

In figure 17 the average time period per iteration that the flow is applied to each of the three chips is shown for the experiment with DI water (A) and cell culture medium (B). Based on the set flow rate of 6 µL/min and the volume injection of 2 µL per iteration per channel, the expected value of these time periods is 20 s. It can be seen that for each position, the average period lies in close proximity to this expected value. For figure 17A, the average period that flow was applied to TSoC 3 deviated most from the expected 20 s out of all three data points, with the highest value out of the three average time periods. This indicates that the average flow rate present in this channel was the lowest, which is in agreement with figure 15. For figure 17B, the average period also deviated most from the expected 20 s for chip 3. The high value of 23 s indicates the flow rate being lowest in this channel, which is in agreement with figure 16. Figure 17 proves that similar flow rates were present in all channels throughout the experiment and that there was no particular chip in which the flow rate deviated significantly from the set flow rate. The approach of sequential parallelization provided steady and identical flow rates in each channel, where all requirements that were set in section 2.2 are met. Therefore, very similar conditions can be created over multiple, parallel channels in future experiments. A similar approach for parallelization was developed, based on these results, with microfluidic chips that later can be integrated in the TOP platform.

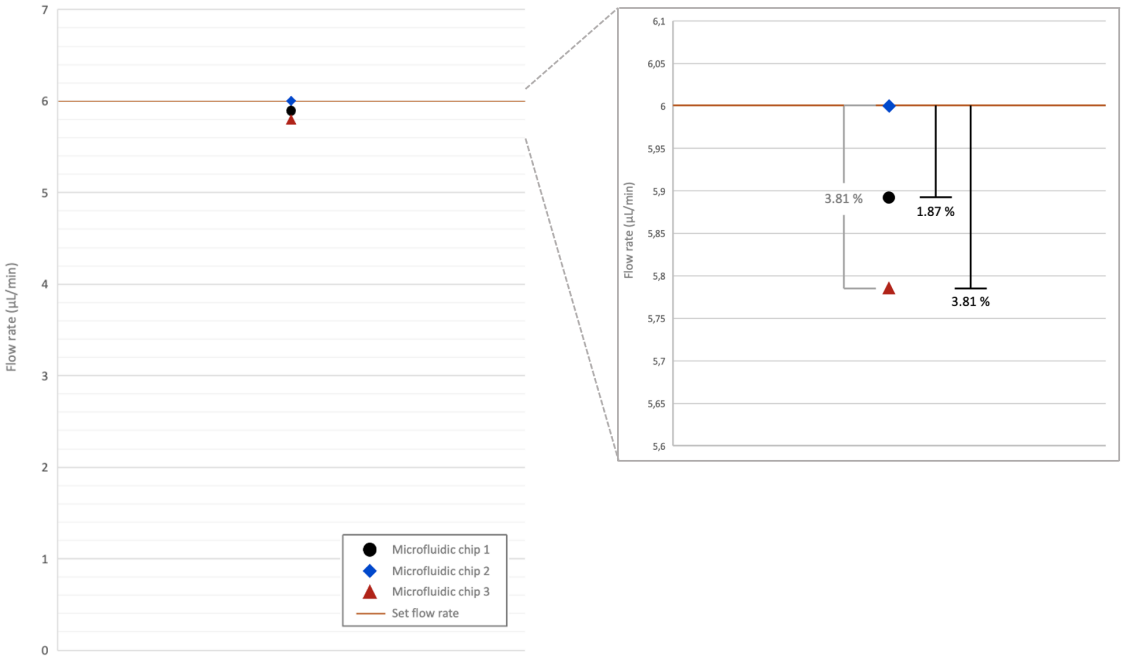

Figure 15: Average flow rate measured in each microfluidic chip and the set flow rate for the experiment with DI water. The percentual difference between the highest and lowest measured value is indicated in grey and the percentual difference between the set flow rate and the measured value per chip is indicated in black.

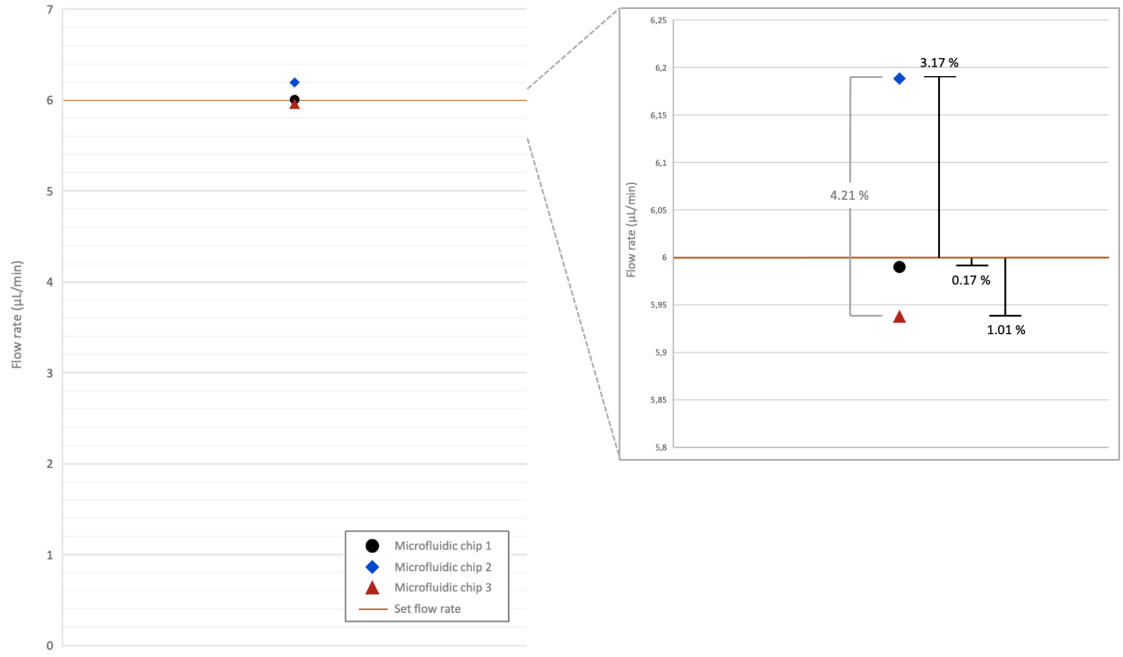

Figure 16: Average flow rate measured in each microfluidic chip and the set flow rate for the experiment with cell culture medium. The percentual difference between the highest and lowest measured value is indicated in grey and the percentual difference between the set flow rate and the measured value per chip is indicated in black.

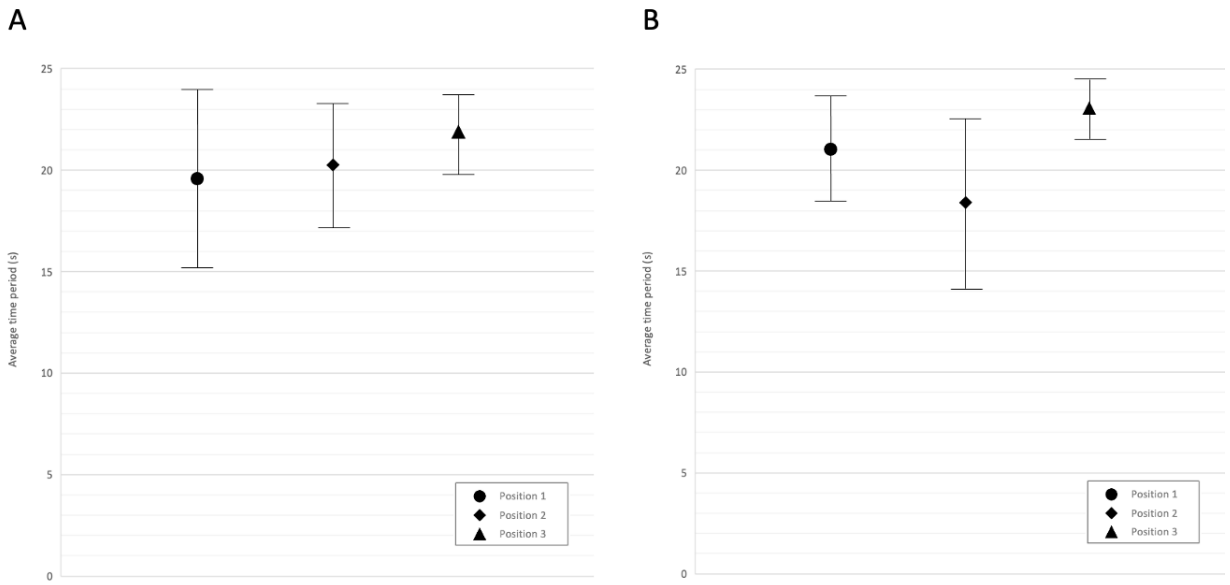

Figure 17: The average period, with standard deviation, that the flow is applied to a certain channel for the experiment with A) DI water and B) cell culture medium. Position 1, 2 and 3 corresponds with the flow being present in microfluidic chip 1, 2 and 3, respectively.

4.2.3 Pneumatic valve characterization

The closing behavior of the pneumatic valves was characterized at different pressures (dP) that were applied to the reservoir to induce flow, and different closing pressures that were applied to the pneumatic valves. For the entire range of pressures applied to the reservoir, the valves were fully closed at a pressure of 1.5 bar. Therefore, a pressure of 1.5 bar was used as the closing pressure while performing experiments with the system.

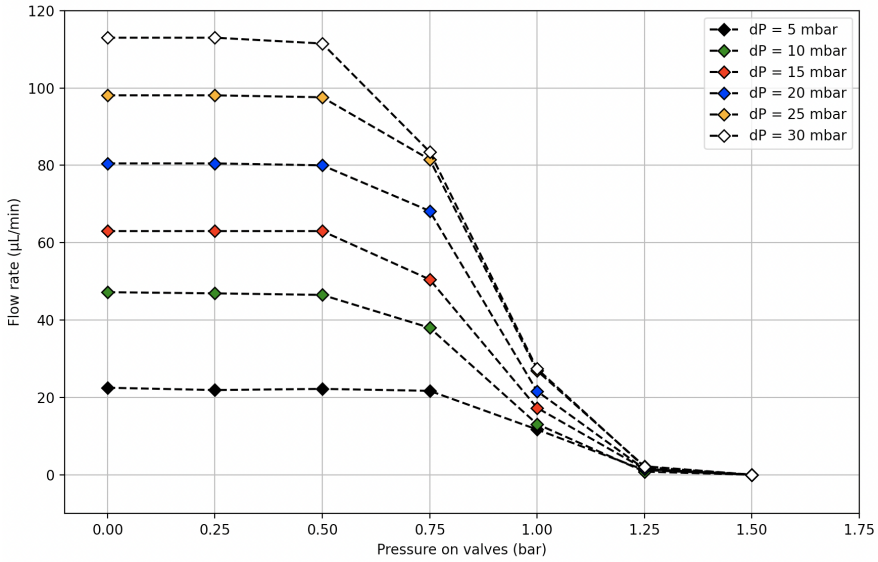

Figure 18: Flow rate plotted against the pressure that is applied to the valve for a total of five differential pressures (dP), where dP is the differential pressure between inlet and outlet of the microfluidic system.

4.2.4 Feedback loop settings for flow parallelization

To test the ideal settings for the PID control loop, multiple PG values were tested by investigating the flow rate profile observed. The value for T_I was set at 0.005 s as this showed the most stable response. the flow rate was set at 10 µL/min and parallelization was performed with the DDC over three channels. The volume after which switching between channels is initiated, was set at 3.5 µL and the flow rate was measured over a total period of six switching times. The flow rate profile for PG values of 0.1 to 0.9 with 0.1 increments is shown in figure 19. The peaks in flow rate indicate switching moments between channels.

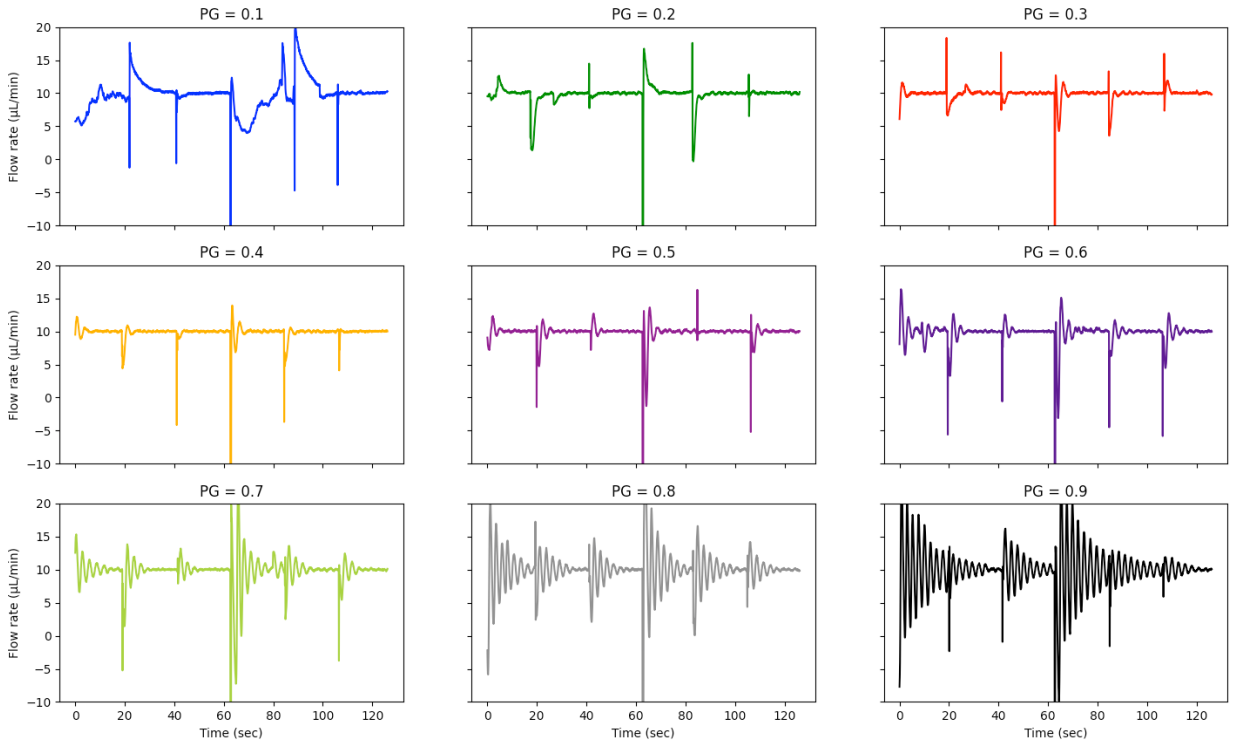

Figure 19: Flow rate profiles for PG values of 0.1 to 0.9 with 0.1 increments.

From figure 19 follows that at the lowest PG value of 0.1, the control loop needs a relatively long time to achieve a steady flow rate of 10 µL/min. The quickness in response is already much improved for PG = 0.2. At PG values of 0.5 and higher, the control loop starts to oscillate after switching between channels. The response becomes increasingly more unstable for higher PG values. From these results the choice was made to make use of a value of PG = 0.4.

4.2.5 Parallelization with microfluidic chips

After successfully parallelizing flow over three microfluidic chips with commercially available equipment, the DDC was developed to replace the M-switch rotary valve. The DDC has one inlet channel that bifurcates into four parallel channels, where each channel can be independently opened or closed with pneumatic valves. In this way, a flow can be parallelized, by sequentially opening the four channels. The DDC can potentially become a new MFBB, to be integrated on the TOP platform. Then, it can fully harness the advantages that the TOP platform offers.

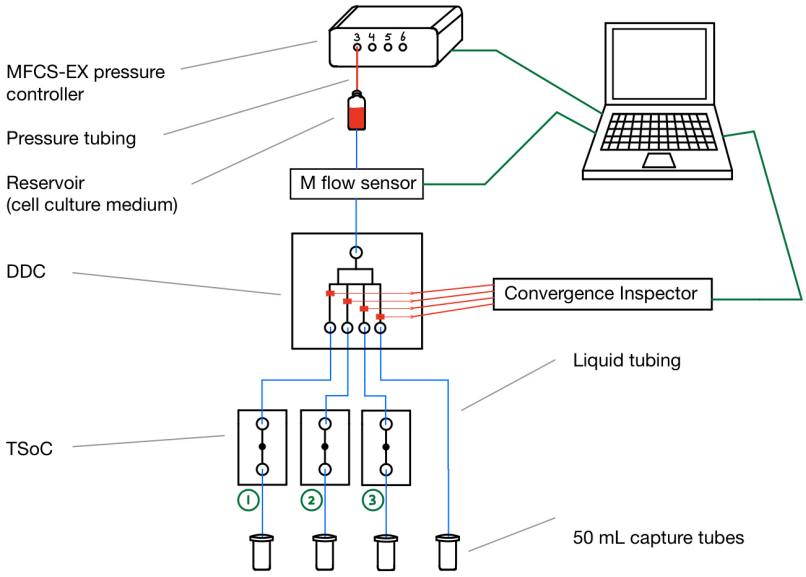

Figure 20: Schematic overview of the setup used for sequential parallelization with microfluidic chips.

To test whether flow can be steadily parallelized using the DDC, the same experiment as performed in section 4.2.2 was performed with the setup shown in figure 20. To three of the four outlets of the DDC, a TSoC was connected. A flow of DI water was sequentially parallelized over the three TSoCs for a period of 72 h at a flow rate of 10 µL/min. The volume after which the flow is switched between channels was set at 3.5 µL, such that each channel was subjected to a flow for approximately 20 s and static conditions for 40 s every iteration.

The average flow rates per channel that were present during parallelization are shown in figure 21. Bigger differences in average flow rate are observed, compared to the experiment performed with commercially available equipment. A 29.58 % difference between the highest and lowest values of observed, which falls outside of the required 10 % maximum difference. This difference can be explained by an increasing delay in loading of the parallelization protocol throughout the duration of the experiment. The parallelization protocol is a sub-program that opens the valves of the three channels in a sequential manner. After the three channels have been sequentially opened, the program is finished, after which it is then immediately repeated. However, is was observed that over time the repetition of this loop is no longer instantaneous. This could be due to the fact that the software has to process an increasing amount of information. This explains the lower average flow rates present in chip 1 and 2, compared to chip 3. Another factor that could have had an influence, is the volume that is displaced when closing the pneumatic valves. The channel has a width of 2 mm and height of 500 µm. Moreover, the pneumatic valve has a width of 2 mm, resulting in a 2 mm by 2 mm area that is covered by the valve. Taking the height and half rounded form of the channel into account, the volume that is displaced every time the valve is closed is approximately 1.57 µL. This could have led to unequal distribution of volumes over the chips. The average flow rate ± standard deviation, determined over all the flow rate data points that were measured by the M flow sensor throughout the experiment, was 9.54 ± 4.21 µL/min, which is within the required range of 50 % standard deviation and in good accordance with the set flow rate. Thus, the flow rate control loop functions steadily.

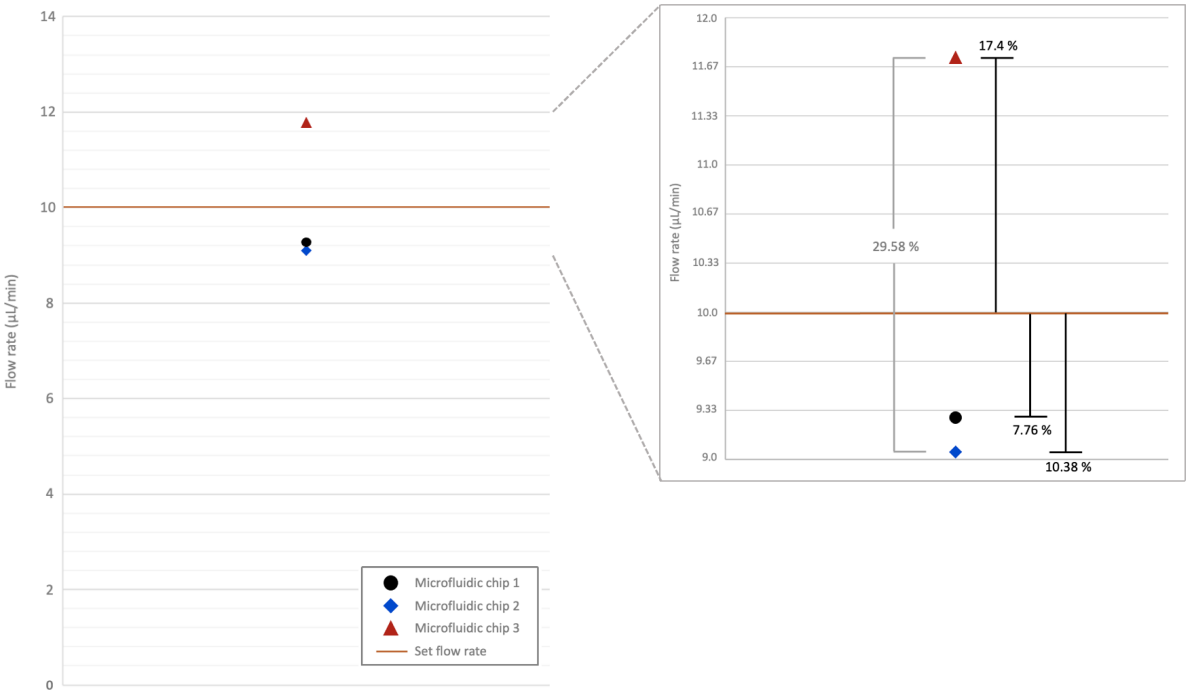

Figure 21: Average flow rate measured in each microfluidic chip and the set flow rate for the experiment. The percentual difference between the highest and lowest measured value is indicated in grey and the percentual difference between the set flow rate and the measured value per chip is indicated in black.

4.3 Generating dynamic concentration profiles on chip

Another main objective of this project was to generate dynamic anti-cancer drug concentration profiles on chip. The concentration profile should be able to cover at least four concentration steps, covering the highest to lowest concentration of a specific drug, where a 50 % reduction in concentration should be realizable within 10 min to mimic drug concentration profiles with a short plasma half-life. The chosen approach for generation of dynamic concentration profiles is based on the approach used by Petreus et al, as discussed in section 1.4. To be able to cover four different concentration steps, four reservoirs were connected to separate ports of the M-switch rotary valve. Each reservoir can be filled with a different concentration of the drug of interest, such that four concentration steps of a certain anti-cancer drug can be covered. In this way, important parameters of the *in vivo* drug concentration profile, AUC and C_{max}, can be matched in a later stage when actual anti-cancer drug concentration profiles will be parallelized.

In the experiment described throughout this section, fluorescein was used as a model for anti-cancer drugs. Due to its ability to emit a fluorescent signal when illuminated and the linear relation between fluorescein concentration and intensity of the emitted light, it is perfectly suitable to investigate whether the supplied concentration steps actually appear on chip.

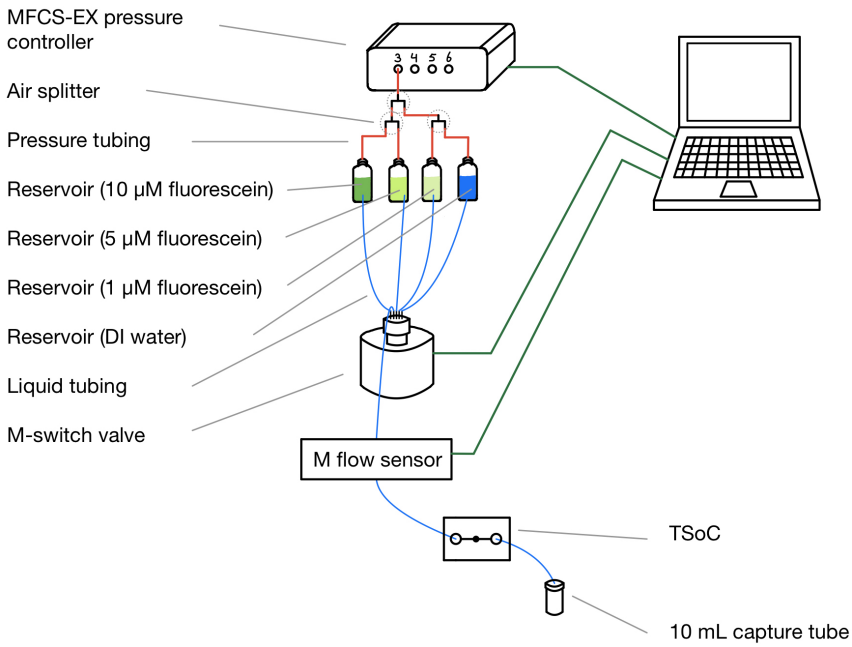

Figure 22: Schematic overview of the setup used for generating a dynamic fluorescein concentration profile on chip.

The setup that was used for the experiment is schematically shown in figure 22. Four concentration steps of fluorescein, with concentrations of 10 µM, 5 µM, 1 µM and 0 µM and a period of 30 min each, were sequentially supplied to one TSoC at a flow rate of 10 µL/min.

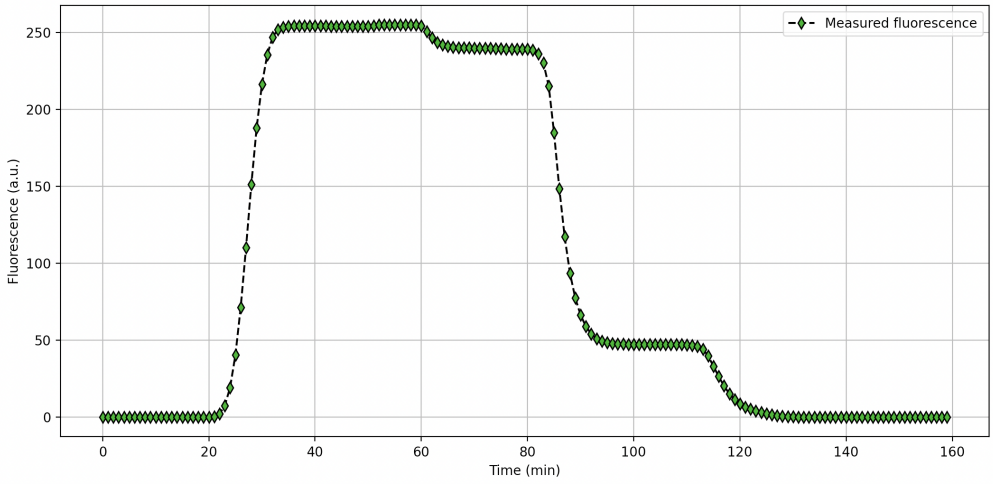

Figure 23: Measured fluorescence intensity of fluorescein for the sequential concentration steps of 10, 5, 1 and 0 µM in the microfluidic chip channel.

The measured fluorescence intensity over time is shown in figure 23. The four concentration are clearly distinguishable and each have a duration of approximately 30 min. The linear dependency between the concentration of fluorescein and the resulting fluorescence intensity is observed between the 0, 1 and 5 µM concentration steps. The 10 µM concentration step fell out of the linear range, but is still distinguishable from the 5 µM step. It can be seen that there is delay between the concentration steps. This is due to the fact that mass transfer in this system is highly convective, which clearly shows from the Peclet number. This is a dimensionless number representing the ratio between convective driven mass transfer and diffusion driven

mass transfer. For this system, the Peclet number is above 300, where a value higher than 1 indicates that convective transport is dominant. The convective driven flow results in a Poiseuille flow profile being present in the microfluidic channels. Poiseuille flow describes the parabolic flow profile that is caused by the friction that is maximum at the walls and the friction between individual flow layers, that decreases when moving from the wall to the centre of the tubing. Therefore, the flow velocity at the walls is zero and increases further from the walls, reaching a maximum at the centre. The concentration of fluorescein being greater at the tubing walls than at the center in the plug's rear end, leads to radial diffusion of fluorescein to the center. Due to the radial diffusion and convection, the parabolic concentration profile spreads in the axial direction. This effect is also referred to as Taylor dispersion [42]. Due to the length that the fluid has to cover to the TSoC, the peak of the parabolic flow profile becomes increasingly sharp over time, as schematically shown in figure 24. Due to the increasing plug, the concentration steps gets smeared out over an increasing distance, resulting in a more gradual build-up to the desired concentration. Nevertheless, the time to achieve a steady concentration is within 10 min between all concentration steps. Thus, the requirement of achieving a 50 % reduction in concentration within 10 min was met. The same holds for the other requirements that were set in section 2.2.

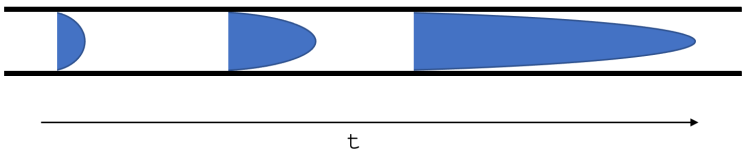

Figure 24: Side view of the increasing plug in flow profile due to Taylor dispersion. Adapted from [43].

It was decided to test the approach for generating dynamic concentration profiles only with commercially available equipment. In section 4.2.5, it was already shown that sequential, parallel distribution was possible with the DDC, using the pneumatic valves. This section proved that the chosen approach for generating dynamic concentration profiles was successful. Therefore, we proceeded with integrating parallelization and generating dynamic drug concentrations without separately testing the DCGC for generating dynamic drug concentrations.

4.4 Integrating parallelization and dynamic drug concentration profiles

4.4.1 Validation experiment with fluorescein

To check whether the system, making use of pneumatic valves for dynamic concentration generation and parallelization (figure 11), is able to generate dynamic drug concentration profiles and supply them to multiple TSoCs, a validation experiment with fluorescein was performed. Four concentration steps of fluorescein, with concentrations of 10 µM, 5 µM, 1 µM and 0 µM and a period of 30 min each, were parallelized over three TSoCs at a flow rate of 10 µL/min. The four 30 min concentration steps were repeated throughout the total duration of the experiment (1000 min).

The measured and expected fluorescence intensity profiles throughout the entire experiment, corrected for dead volume, are shown in figure 25. Throughout the experiment, a total of six concentration step cycles were parallelized over the three TSoC. Five of the six cycles closely follow the trend of the expected fluorescence. During the third cycle, the first concentration step of 10 µM fluorescein does not appear. This is most likely caused by an error in the valves of the DCGC, leaving the channel connected to the fourth concentration step open for two consecutively time periods, thereby skipping the first concentration step of the third cycle. The 5, 1 and 0 µM concentration steps are still present during the third cycle. Apart from this, figure 25 shows that it is possible to parallelize a dynamic concentration profile over multiple TSoCs.

In figure 26, the measured and expected fluorescence intensity profile is shown in more detail for the first cycle of four concentration. It can be seen that the four concentration steps are clearly distinguishable. The expected linear relation between fluorescein concentration and fluorescence intensity is closely followed by measured intensity profile, with a factor difference of 1.6 between the 10 and 5 µM concentration step and a

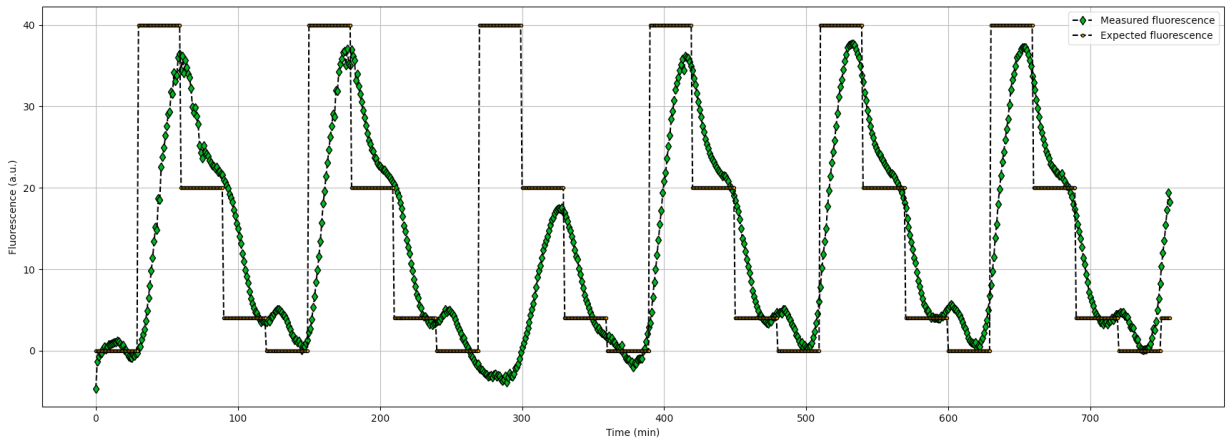

Figure 25: Measured and expected fluorescence intensity of fluorescein for a total of six concentration step cycles, where each cycle has four sequential 30 min concentration steps of 10, 5, 1 and 0 µM. Fluorescence was measured in the microfluidic channel of the TSoC (chip 1).

factor difference of 5.5 between the 5 and 1 µM concentration step. The peak value of the measured profile is 8.88 % lower that the expected peak value. In addition, the area under the AUC of the measured profile is only 6.53 % lower than that of the expected profile. Therefore, two important parameters of the measured concentration profile, C_{max} and AUC, closely match the expected profile. Even though all concentration steps clearly appear in the measured fluorescence graph, there is a greater delay in achieving a steady concentration compared to the profile that was observed in figure 23. A build-up time of approximately 30 min is observed between concentration steps 0 and 10 µM, whereas this was 10 min when generating this concentration profile on a single TSoC. This is due to the increasing plug, caused by Taylor dispersion, as was discussed in section 4.3. In this experiment the flow rate was also set at 10 µL/min. However, the effective flow rate is reduced by a factor three in the tubing leading to the TSoCs, as the flow is sequentially parallelized over three separate TSoCs. Therefore, the build-up time is increased by the same factor three. The build-up time between concentrations can be reduced by decreasing the tubing length. Relatively long tubing was needed for this experiment to be able to image the TSoC under the microscope. In the experiment with oxaliplatin, the concentration profile is anticipated to follow the expected concentration profile more closely, due to the tubing length being shorter. After the first concentration step of 10 µM, the fluorescence profile follows the expected trend more closely, if accounted for the 30 min build-up time during the first concentration step. A 50 % reduction in concentration was achieved in approximately 10 min between all concentration steps, as required.

To validate whether the fluorescein concentration profile was parallelized equally over the three TSoCs, the waste of the volume that passed through the individual chips was analysed for fluorescence intensity. The results are shown in figure 27A. As a reference, the intensities of the four concentration steps are included in the same well plate at equal volume. The intensities measured for the three TSoCS lie in close proximity of each other, indicating that each chip received the same concentration steps. Based on the six concentration cycles that have been completed and correcting for the dead volume of water that was present in the system before start of the experiment, the expected concentration of fluorescein in the waste of each chip is approximately 3 µM. This corresponds to a fluorescence intensity of 27 a.u. The measured intensities (± standard deviation) for TSoC 2 and 3 are in accordance with this expected value. The value for TSoC 1 is slightly lower. Figure 27B shows the volumes of the captured waste per TSoC. Based on the duration of 1000 min and a flow rate of 10 µL/min divided over three chips, the expected captured volume per TSoC is 3.33 mL. It becomes apparent that the volume that passed through TSoC 1 was slightly lower than the captured volumes of TSoC 2 and 3, which could have led to unequal distribution of the four concentration steps and might explain the lower fluorescence intensity that was measured for TSoC 1.

The results obtained in this experiment show that it is possible to steadily parallelize a dynamic concen-

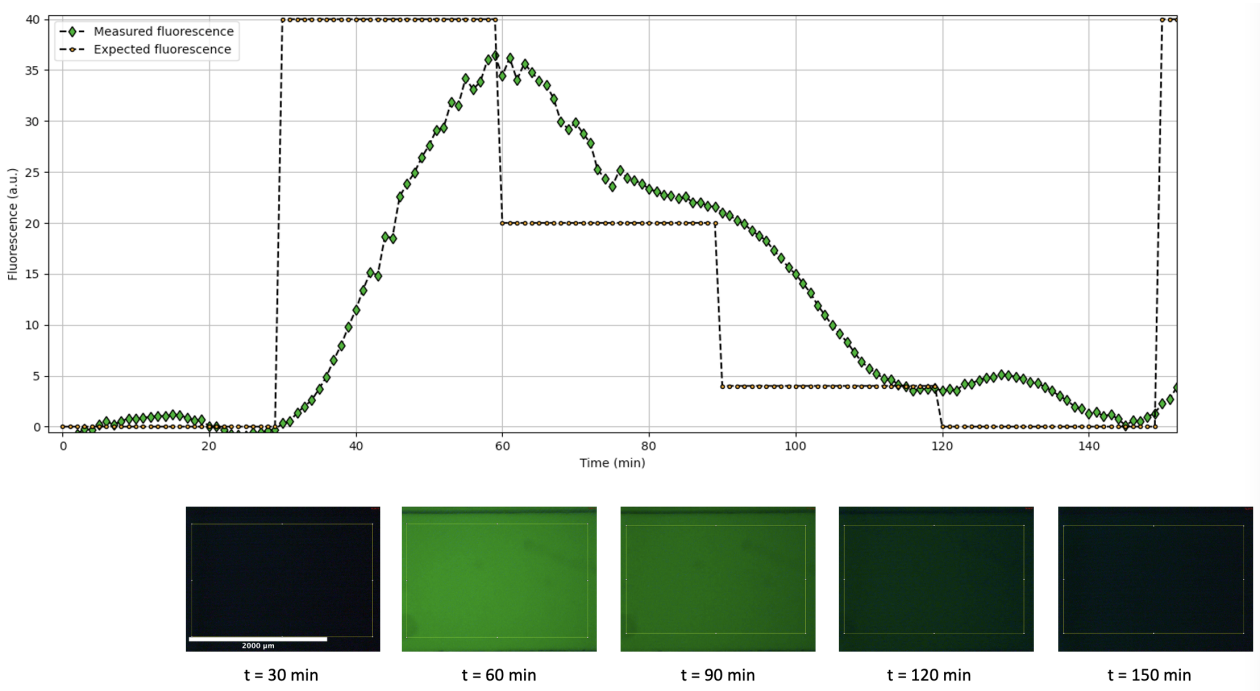

Figure 26: Measured and expected fluorescence intensity of fluorescein for the first cycle of sequential 30 min concentration steps of 10, 5, 1 and 0 µM, in the microfluidic channel of the TSoC (chip 1). Images used for fluorescence analysis, with marked analysis area (yellow square), are shown below the graph at specific time points. Scale bar is 2 mm.

tration profile over three TSoCs with the system introduced in section 4.1.

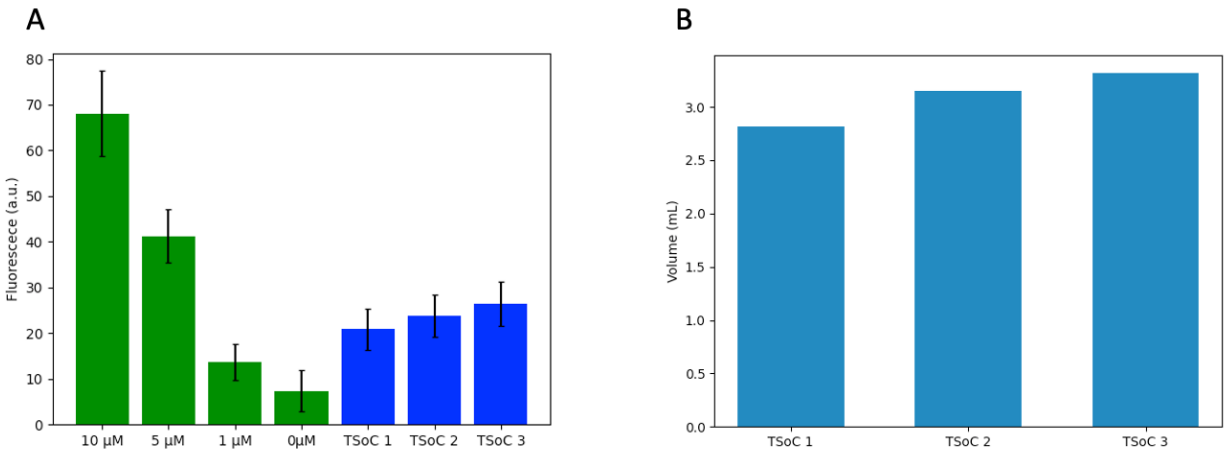

Figure 27: A) The fluorescence intensity measured for the fluorescein concentration steps (green) and the waste of the three TSoCs (blue), with standard deviation of the individual pixels in the analyzed area. Fluorescence intensity was measured in separate wells of a 96-well plate. B) The total volume of the captured waste per TSoC.

4.4.2 Investigating spheroid growth on parallel TSoCs

For the system, designed throughout this project (figure 4.1), to be used for performing parallel testing of anti-cancer drugs on tumour spheroids, the spheroids need to be able to grow on the TSoCs. Throughout the experiment the flow of culture medium is sequentially parallelized, where every minute each spheroid is

subjected to a flow for 20 s and to static conditions for 40 s. It was decided to use flow rates of around 6 to 10 µL/min, resulting in an effective flow rate of 2 or 3.33 µL/min per channel, respectively. In this way, the volume above the spheroid culture well in the TSoC is refreshed during every iteration. Moreover, these flow rates are high enough to maintain a stable flow rate over time and low enough to prevent the spheroids from being flushed out of the well. Therefore, these flow rates are deemed more than sufficient for maintaining proper culture conditions on chip during sequential parallelization. [44]

To investigate spheroid growth on chip, spheroids were seeded in the wells of three TSoCs and connected to the rest of the system shown in figure 11. McCoy 5A cell culture medium was sequentially supplied to the three TSoCs at a flow rate of 10 µL/min. The percentual growth in volume of the spheroids was determined over a period of 48 h.

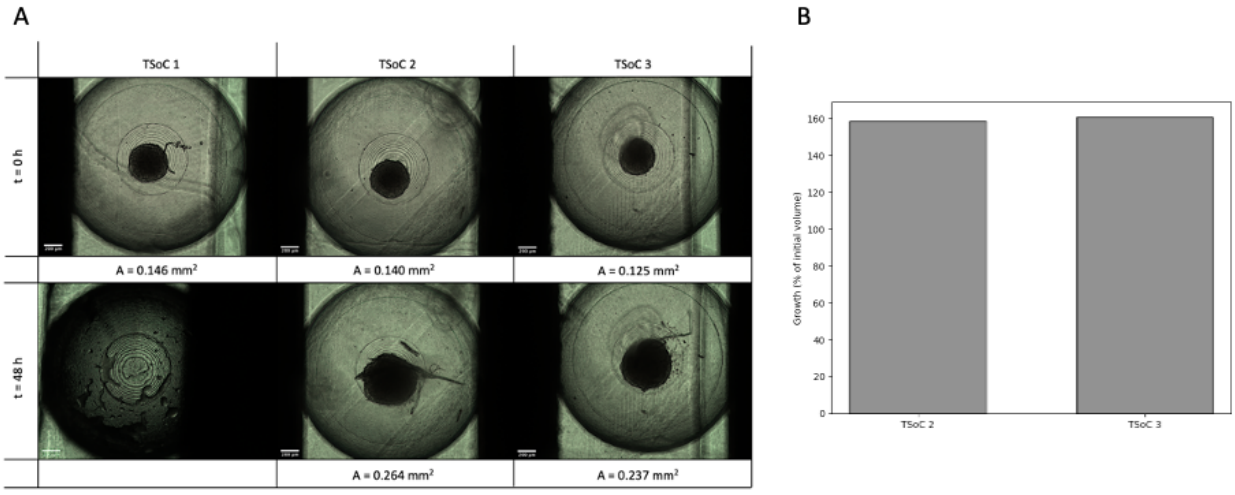

Figure 28: A) Images of the tumour spheroids (HCT-116) on TSoC 1, 2 and 3 at t = 0 h and t = 48 h. For each spheroid the surface area is given in mm^2. Scale bar is 200 µm. B) Percentual growth of the spheroids on TSoC 2 and 3 relative to initial spheroid volume at t = 0.

Images of the spheroids with corresponding surface area at t = 0 h and t = 48 h are shown in figure 28A. Spheroid sizes at t = 0 s correspond well with the spheroid growth kinematics found in literature. After four days of static culture in Thermo Scientific Nunclon Sphera 96-well U-bottom plates, at a seeding density of 2000 cells, the expected spheroid diameter is approximately 400-500 µm, which corresponds with the diameters of the spheroids in TSoC 1, 2 and 3 at t = 0 s [45]. The percentual growth over 48 h for was 158.88% and 161.02 % for TSoC and 3, respectively (see figure 28B). Growth could not be determined for TSoC 1, as the spheroid was likely flushed out of the well when removing tubing after the experiment. The observed growth rate of the spheroids is higher than growth rates found in literature for spheroids cultured in static conditions, which lie around 80 - 100 % [45]. The higher growth rates observed in this experiment might be explained by the fact that the spheroids were exposed to a dynamic flow of culture medium as opposed to static culture conditions. These results prove that with this system it is possible for the spheroids to proliferate and grow under sequential, parallel flow.

4.4.3 Parallelization of the dynamic *in vivo* oxaliplatin concentration profile

As a final test for the system (figure 11) to be used as an *in vitro* model for testing chemotherapies in parallel, the *in vivo* concentration profile of oxaliplatin was parallelized over three TSoCs. Oxaliplatin is a type of anti-cancer drug, classified as an alkylating agent, aimed at treating colorectal cancer [46], [47]. The spheroids used in this research consist of HCT-116 colorectal cancer cells, therefore oxaliplatin serves as an adequate model drug. For this experiment, three spheroids were placed in series in each TSoC, thereby scaling up the experiment significantly. It was shown earlier by Komen et al, that three spheroids placed in series on one chip show equal growth to a single spheroid on chip. This can be seen in figure 39 in appendix C.

The *in vivo* concentration profile of oxaliplatin in mice and the four concentration steps used in this experiment are shown in figure 29. The concentration steps were chosen such that the peak concentration and the area under the curve (AUC) of the *in vivo* profile are matched. The peak value (9 µM) was set slightly higher than the *in vivo* peak concentration to account for Taylor dispersion, resulting in lowering of the initial peak value that was observed in the fluorescein validation experiment. The flow rate was set at a value of 6 µL/min, resulting in an effective flow rate of 2 µL/min per channel. This specific flow rate was chosen as previous experiments performed by Komen et al also used a flow rate of 2 µL/min.

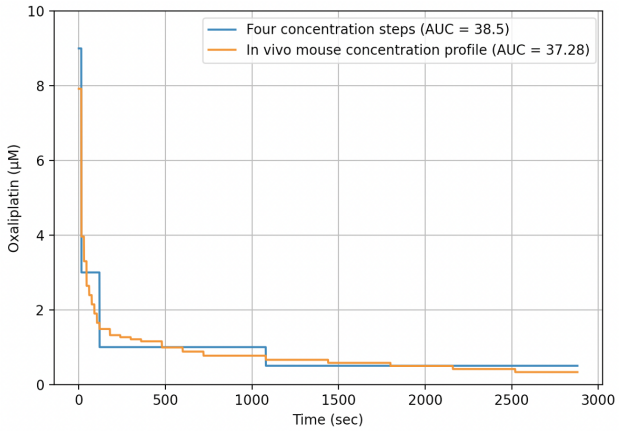

Four concentration steps

Time (min)	Oxaliplatin (µM)
15	9
105	3
960	1
1800	0,5

Figure 29: *In vivo* concentration profile (orange) measured by mass spectrometry in mice blood plasma at 15, 30 min, 1, 2, 3, 4, 8, 10, 24 and 48 hr after intravenous dosing of oxaliplatin (8 mg/kg) [48]. The four concentration steps, representing the *in vivo* mouse concentration profile (blue), with a table showing the concentration steps in more detail.

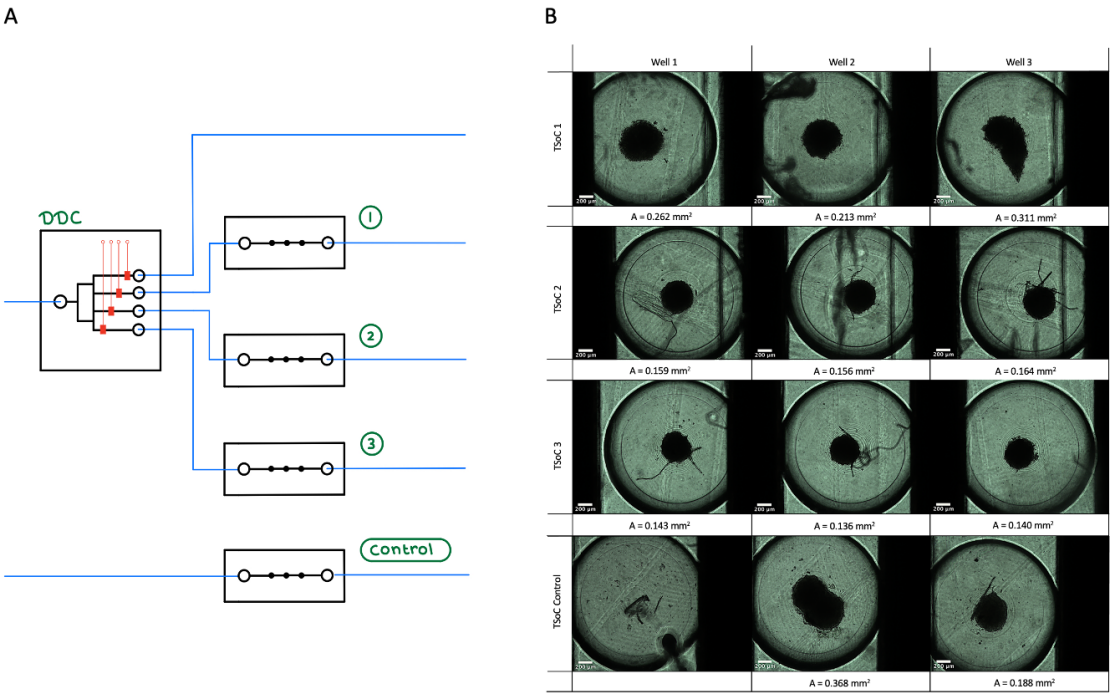

Figure 30: A) Schematic overview of the three TSoCs that were treated with the *in vivo* concentration profile of oxaliplatin and the control TSoC. B) Images of the spheroids (HCT-116) on TSoC 1, 2, 3 and control at t = 48 h. For each spheroid, the surface area is given in mm^2. Scale bar is 200 µm.

When setting up the experiment, several observations were made. The spheroid in control TSoC well 1 was flown out into well 2, due to the top part of the TSoC that had to be replaced, as the chip was leaking initially. In addition, the spheroid in control TSoC well 3 appeared to be less dense and less round than most of the spheroids in the other wells. Lastly, the spheroid in TSoC 1 well 3 was irregular in form. The rest of the spheroids were equal in size, roundness and density. Images of the spheroids at t = 0 h are shown in figure 40 in appendix C.

A schematic overview of the treated TSoCs and control TSoC, with images of the corresponding spheroids at t = 48 h are shown in figure 30. It can be seen that the spheroids in TSoC 1 appeared to have grown more than the spheroids in TSoC 2 and 3. Additionally, the spheroids in the control TSoC appear to have grown less than the growth (158.88 % and 161.02 %), that were observed in section 4.4.2, where spheroids were exposed to cell culture medium over a period of 48 h. This is due to two spheroids being present in well 2 of the control TSoC, leading to less growth over time. Moreover, the spheroid in well 3 of the control TSoC did not have the ideal shape and density, as discussed earlier, which might have led to less growth.

The average growth of the spheroids in TSoC 1, 2 and 3 was compared to the average growth of the untreated spheroids, that was observed in section 4.4.2. This decision was made because the control TSoC was deemed inadequate to use as a control, due to the problems that originated at the start of the experiment, as discussed above. The average growth of the spheroids in TSoC 1, 2 and 3, compared to the average growth that was observed in section 4.4.2, is shown in figure 31A. It can be seen that growth inhibition was observed in all three TSoCs. However, growth inhibition appears to be greatest for TSoC 3 and lowest for TSoC 1. This indicates that TSoC 1 was exposed to a lower amount of oxaliplatin than TSoC 2 and 3. In the validation experiment with fluorescein a similar observation was made, where a lower fluorescein concentration was present in the captured waste of TSoC 1, compared to TSoC 2 and 3. This can be due to the higher flow rate present in TSoC 3, compared to TSoC 1 and 2, throughout the experiment. This was also the case for this experiment, as the captured volume for TSoC 3 was larger by approximately 20 % than the captured volume for TSoC 1 and 2 (figure 31B). This reoccurring problem can be traced back to the results obtained in section 4.2.5, where a larger average flow rate was present in microfluidic chip 3, compared to chip 1 and 2. The higher relative flow rate observed in TSoC 3 can have led to an unequal distribution of oxaliplatin over the three chips, leading to a lower exposure in TSoC 1, resulting in a lower growth inhibition.

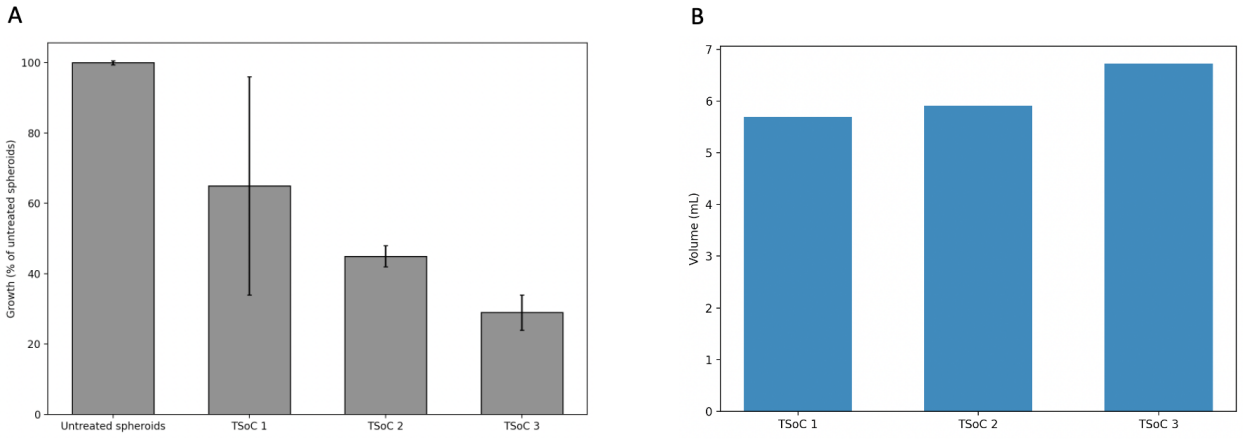

Figure 31: A) Average 48 hour spheroid growth relative to untreated spheroids (growth obtained from experiment in section 4.4.2) for TSoC 1, 2 and 3. Error bars indicate the standard deviation. N = 3 for TSoC 1,2 and 3, N = 2 for untreated spheroids. B) The captured volume that has flown through TSoC 1,2 and 3.

4.5 Integration of the system on the TOP platform

The aim at the start of this project was to develop microfluidic chips that can be integrated on the TOP platform, with which parallel testing of *in vivo*-like anti-cancer drug concentrations on tumour spheroids can be performed. The limited time that was available for this project and challenges in experiment duration and robustness, did not allow for actually integrating the developed chips on the TOP platform. However, a potential first setup to achieve this was developed, which is shown in figure 32, consisting of two parallelization chips (right and left) and one spheroid chip (middle) on which a total of 18 spheroids can be placed.

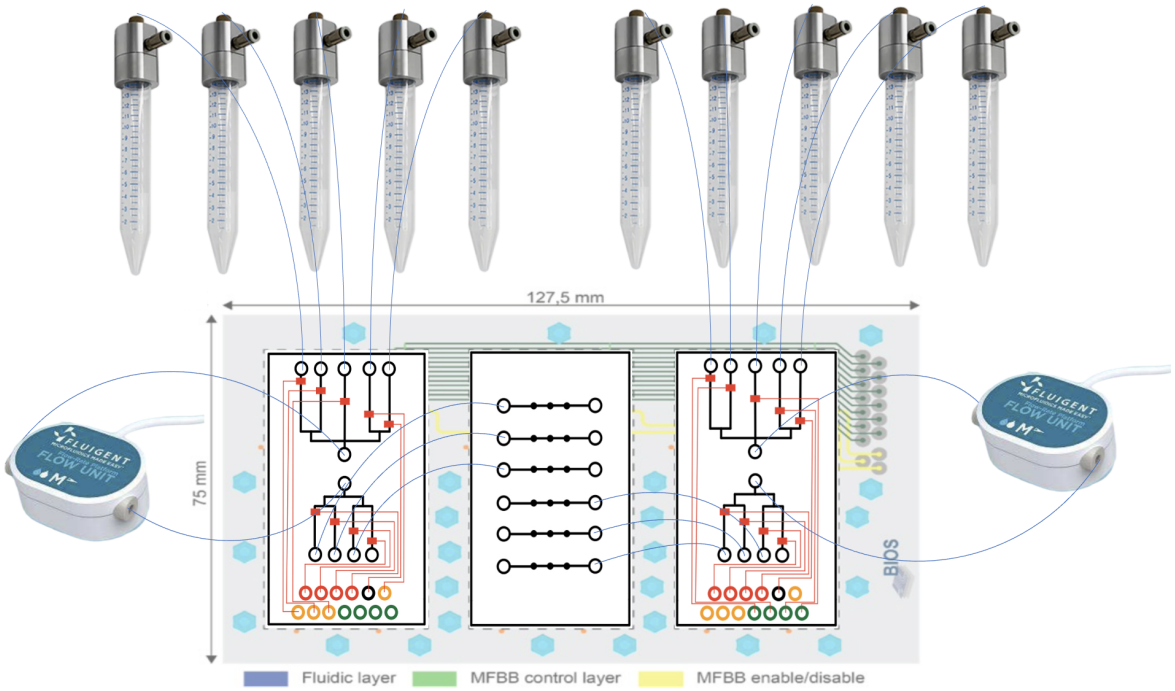

Figure 32: Schematic overview of the parallelization MFBBs integrated on the FCB.

In this setup, the DDC and DCGC are combined into one parallelization chip, with the addition of one more inlet channel. The five inlet channels are not directly connected to the four outlet channels, but each lead to a separate in- and outlet, such that a M flow sensor can be placed in between with which the flow control loop can be created. The pneumatic valves on the two parallelization chips can be controlled from the 13 inlets in the right-top corner of the FCB. The advantage of this is that the pneumatic valves of the four parallelization channels (indicated by the red circle) on both chips can be controlled simultaneously from the same four inlets on the FCB. The pneumatic valves of four out of five inlet channels can be controlled with the inlets indicated in orange for the left parallelization chip and with the inlets indicated in green for the the right parallelization chip. In this way, separate dynamic drug concentration profiles can be generated with both chips. The pneumatic valve on one of the inlet channels on both parallelization chips is connected to the same inlet, which is indicated in black. With this channel, the chips can be flushed simultaneously with water, detergent or alcohol before and after experiments to easily clean the system. Three of the four outlet channels of both parallelization chips are connected to the channels on the spheroid chip. The other outlet channel is used as a waste channel, as was done throughout this project. This design was specifically made to fit on the FCB that was designed at BIOS Lab-on-a-chip group, however, a new FCB design could be developed specifically for parallelization of dynamic drug concentration profiles. The DDC that was developed can also be used for parallelization of other types of experiments, such as serial supply of different stem cell differentiation culture media, for which project are currently conducted by BIOS and the AST group.

5 Conclusions and outlook

5.1 Conclusions

In this research a novel microfluidic system was designed, manufactured and tested, with which dynamic, *in vivo*-like, anti-cancer drug concentrations were sequentially parallelized over three parallel microfluidic channels, using TOP compatible pneumatic valves. The validation experiment, where fluorescein was used as a model drug, showed that four concentration steps of 10, 5, 1 and 0 µM were successfully parallelized over three parallel microfluidic chips. Moreover, tumour spheroids were able to grow on chip, during sequential parallelization of cell culture medium, where the spheroids, in two of the three chips, showed a percentual growth of 158.88 % and 161.02 % over a period of 48 h. Finally, with this system, three microfluidic chips, accommodating tumour spheroids, could be exposed to the *in vivo* oxaliplatin concentration profile. Lower growth was found, when exposing spheroids to the *in vivo* oxaliplatin concentration profile, compared to the growth that was found in untreated spheroids in a separate experiment. However, further validation of these results is needed due to the high variability and disrupted growth in the control chip of the same experiment.

5.2 Outlook

To further validate this system as an adequate *in vitro* model for parallel testing of anti-cancer drugs, more experiments with different types of anti-cancer drugs need to be performed and compared to outcomes found in mouse studies. When the system proves to be able to replicate those outcomes, efforts can be made in further upscaling of the system by integrating the microfluidic chips, designed throughout this project, on the FCB that was shown in section 1.4.2. A potential first setup to achieve this was shown in figure 32.

It is recommended to make changes to the channel dimensions of the DDC. Now a channel width of 2 mm and height of 500 µm is used. Moreover, the pneumatic valve has a width of 2 mm, resulting in a 2 mm by 2 mm area that is covered by the valve. As was already discussed in section 4.2.5, this leads to high volume displacement when closing the valve. As this happens almost instantaneously, this causes sudden deviations in flow rate, thereby making the system unstable. This can cause more volume to flow through the channels than is desired. Decreasing the width of the channel and the pneumatic valves by a factor 4, would already result in a factor 16 decrease in the volume displacement that occurs when closing the valve.

Throughout this project the software that was used is still in development and proved to be unstable at times, when performing relatively long experiments of 48 h or longer. For this system to be used for extensive testing of different anti-cancer drugs, the stability of the software should be improved.

In the experiments that were performed with tumour spheroids, the spheroids had to be manually pipetted into the culture well of the TSoC. A useful improvement to the current experimental procedure would be the possibility to seed and grow spheroids on chip.

6 Acknowledgements

First of all, I would like to thank Job Komen for the support and daily supervision throughout this project. Thank you for always being approachable and available, and for the weekly meetings where we had nice discussions. Thank you, Elsbeth, for helping me with the microfluidic chip design and production. Your help in the lab has been very useful.

I want to express my gratitude to Albert van den Berg and Andries van der Meer for taking part in my graduation committee and the evaluation of my master thesis.

A special thanks to Felix Broens from Convergence, who provided me the software that was used for a large part of this project and protocols to run the experiments.

Last but certainly not least, I want to thank all of the BIOS Lab-on-a-chip group for providing me a pleasant working environment.

References

[1] *Cancer*. URL: https://www.who.int/news-room/fact-sheets/detail/cancer.

[2] *Cancer treatment - Mayo Clinic*.
URL: https://www.mayoclinic.org/tests-procedures/cancer-treatment/about/pac-20393344.

[3] Vincent T. DeVita and Edward Chu. "A History of Cancer Chemotherapy".
In: *Cancer Research* 68.21 (Nov. 2008), pp. 8643–8653. ISSN: 0008-5472.
DOI: 10.1158/0008-5472.CAN-07-6611.
URL: https://aacrjournals.org/cancerres/article/68/21/8643/541799/A-History-of-Cancer-Chemotherapy.

[4] *Cancer treatment statistics — Cancer Research UK*.
URL: https://www.cancerresearchuk.org/health-professional/cancer-statistics/treatment#heading-Four.

[5] Jihoon Ko et al. "Tumor spheroid-on-a-chip: a standardized microfluidic culture platform for investigating tumor angiogenesis". In: *Lab on a Chip* 19.17 (Aug. 2019), pp. 2822–2833.
ISSN: 14730189. DOI: 10.1039/C9LC00140A.
URL: https://pubs.rsc.org/en/content/articlehtml/2019/lc/c9lc00140a%20https://pubs.rsc.org/en/content/articlelanding/2019/lc/c9lc00140a.

[6] *Establishing the scientific validity of complex in vitro models - Publications Office of the EU*.
URL: https://op.europa.eu/es/publication-detail/-/publication/3824b024-5621-11eb-b59f-01aa75ed71a1.

[7] *NCI-60 Screening Methodology — NCI-60 Human Tumor Cell Lines Screen — Discovery & Development Services — Developmental Therapeutics Program (DTP)*.
URL: https://dtp.cancer.gov/discovery_development/nci-60/methodology.htm.

[8] Bárbara Pinto et al.
"Three-Dimensional Spheroids as In Vitro Preclinical Models for Cancer Research".
In: *Pharmaceutics 2020, Vol. 12, Page 1186* 12.12 (Dec. 2020), p. 1186.
DOI: 10.3390/PHARMACEUTICS12121186. URL: https://www.mdpi.com/1999-4923/12/12/1186/htm%20https://www.mdpi.com/1999-4923/12/12/1186.

[9] Kristina V. Kitaeva et al. "Cell Culture Based in vitro Test Systems for Anticancer Drug Screening".
In: *Frontiers in Bioengineering and Biotechnology* 0 (Apr. 2020), p. 322. ISSN: 2296-4185.
DOI: 10.3389/FBIOE.2020.00322.

[10] *Medical Writing — Preclinical Studies — Preclinical research in drug development*. URL: https://journal.emwa.org/preclinical-studies/preclinical-research-in-drug-development/.

[11] *US cancer institute overhauls cell lines: veteran cells to be replaced by human tumours grown in mice - Document - Gale Academic OneFile*.
URL: https://go.gale.com/ps/i.do?id=GALE%7CA444595385&sid=googleScholar&v=2.1&it=r&linkaccess=abs&issn=00280836&p=AONE&sw=w&userGroupName=anon%7E73524983.

[12] Ryo Tsumura et al. "Report of the use of patient-derived xenograft models in the development of anticancer drugs in Japan". In: *Cancer Science* 111.9 (Sept. 2020), pp. 3386–3394. ISSN: 1349-7006.
DOI: 10.1111/CAS.14564.
URL: https://onlinelibrary.wiley.com/doi/full/10.1111/cas.14564%20https://onlinelibrary.wiley.com/doi/abs/10.1111/cas.14564%20https://onlinelibrary.wiley.com/doi/10.1111/cas.14564.

[13] Dongeun Huh, Geraldine A. Hamilton, and Donald E. Ingber.
"From 3D cell culture to organs-on-chips". In: *Trends in Cell Biology* 21.12 (Dec. 2011), pp. 745–754.
ISSN: 0962-8924. DOI: 10.1016/J.TCB.2011.09.005.

[14] Ping Cui and S. Wang.
"Application of microfluidic chip technology in pharmaceutical analysis: A review".
In: *Journal of Pharmaceutical Analysis* 9.4 (Aug. 2019), pp. 238–247. ISSN: 2095-1779.
DOI: 10.1016/J.JPHA.2018.12.001.

[15] Sangeeta N. Bhatia and Donald E. Ingber. "Microfluidic organs-on-chips".
In: *Nature Biotechnology 2014 32:8* 32.8 (Aug. 2014), pp. 760–772. ISSN: 1546-1696.
DOI: 10.1038/nbt.2989. URL: https://www.nature.com/articles/nbt.2989.

[16] Mira Stadler et al. "Increased complexity in carcinomas: Analyzing and modeling the interaction of human cancer cells with their microenvironment".
In: *Seminars in Cancer Biology* 35 (Dec. 2015), pp. 107–124. ISSN: 1044-579X.
DOI: 10.1016/J.SEMCANCER.2015.08.007.

[17] Kamila Białkowska et al. "Spheroids as a Type of Three-Dimensional Cell Cultures—Examples of Methods of Preparation and the Most Important Application".
In: *International Journal of Molecular Sciences* 21.17 (Sept. 2020), pp. 1–17.
DOI: 10.3390/IJMS21176225.
URL: /pmc/articles/PMC7503223/%20/pmc/articles/PMC7503223/?report=abstract%20https://www.ncbi.nlm.nih.gov/pmc/articles/PMC7503223/.

[18] Elisabete C. Costa et al.
"3D tumor spheroids: an overview on the tools and techniques used for their analysis".
In: *Biotechnology Advances* 34.8 (Dec. 2016), pp. 1427–1441. ISSN: 0734-9750.
DOI: 10.1016/J.BIOTECHADV.2016.11.002.

[19] "Glossary Collection of terms, symbols, equations, and explanations of common pharmacokinetic and pharmacodynamic parameters and some statistical functions". In: (2004).

[20] *Dosing of anticancer agents in adults - UpToDate*.
URL: https://www.uptodate.com/contents/dosing-of-anticancer-agents-in-adults/print.

[21] Brooke Schuster et al.
"Automated microfluidic platform for dynamic and combinatorial drug screening of tumor organoids".
In: *Nature Communications 2020 11:1* 11.1 (Oct. 2020), pp. 1–12. ISSN: 2041-1723.
DOI: 10.1038/s41467-020-19058-4.
URL: https://www.nature.com/articles/s41467-020-19058-4.

[22] Christian Lohasz et al. "Tubing-Free Microfluidic Microtissue Culture System Featuring Gradual, in vivo-Like Substance Exposure Profiles".
In: *Frontiers in Bioengineering and Biotechnology* 0.APR (2019), p. 72. ISSN: 2296-4185.
DOI: 10.3389/FBIOE.2019.00072.

[23] Tudor Petreus et al. "Tumour-on-chip microfluidic platform for assessment of drug pharmacokinetics and treatment response". In: *Communications Biology 2021 4:1* 4.1 (Aug. 2021), pp. 1–11.
ISSN: 2399-3642. DOI: 10.1038/s42003-021-02526-y.
URL: https://www.nature.com/articles/s42003-021-02526-y.

[24] Yadir A. Guerrero et al. "A Microfluidic Perfusion Platform for In Vitro Analysis of Drug Pharmacokinetic-Pharmacodynamic (PK-PD) Relationships".
In: *The AAPS Journal 2020 22:2* 22.2 (Mar. 2020), pp. 1–10. ISSN: 1550-7416.
DOI: 10.1208/S12248-020-0430-Y.
URL: https://link.springer.com/article/10.1208/s12248-020-0430-y.

[25] Yaqiong Guo et al.
"Modeling Pharmacokinetic Profiles for Assessment of Anti-Cancer Drug on a Microfluidic System".
In: *Micromachines 2020, Vol. 11, Page 551* 11.6 (May 2020), p. 551. DOI: 10.3390/MI11060551.
URL: https://www.mdpi.com/2072-666X/11/6/551/htm%20https://www.mdpi.com/2072-666X/11/6/551.

[26] George A. Truskey.
"Human Microphysiological Systems and Organoids as in Vitro Models for Toxicological Studies".
In: *Frontiers in Public Health* 6 (July 2018), p. 185. ISSN: 22962565.
DOI: 10.3389/FPUBH.2018.00185/BIBTEX.

[27] Kirsten Fetah et al. "High throughput physiological micro-models for in vitro pre-clinical drug testing: a review of engineering systems approaches".
In: *Progress in Biomedical Engineering* 2.2 (May 2020), p. 022001. ISSN: 2516-1091.
DOI: 10.1088/2516-1091/AB7CC4. URL: https://iopscience.iop.org/article/10.1088/2516-1091/ab7cc4%20https://iopscience.iop.org/article/10.1088/2516-1091/ab7cc4/meta.

[28] Job Komen et al. "Controlled pharmacokinetic anti-cancer drug concentration profiles lead to growth inhibition of colorectal cancer cells in a microfluidic device".
In: *Lab on a Chip* 20.17 (Aug. 2020), pp. 3167–3178. DOI: 10.1039/D0LC00419G.

URL: https://pubs.rsc.org/en/content/articlehtml/2020/lc/d0lc00419g%20https://pubs.rsc.org/en/content/articlelanding/2020/lc/d0lc00419g.

[29] *Translational Organ-on-Chip Platform - TOP: Translational Organ-on-Chip Platform.* URL: https://top.hdmt.technology/.

[30] A. R. Vollertsen et al. "Modular operation of microfluidic chips for highly parallelized cell culture and liquid dosing via a fluidic circuit board". In: *Microsystems & Nanoengineering 2020 6:1* 6.1 (Nov. 2020), pp. 1–16. ISSN: 2055-7434. DOI: 10.1038/s41378-020-00216-z. URL: https://www.nature.com/articles/s41378-020-00216-z.

[31] Anke R Vollertsen et al. "STANDARDIZED, MODULAR PARALLELIZATION PLATFORM FOR MICROFLUIDIC LARGE-SCALE INTEGRATION CELL CULTURING CHIPS". In: (). URL: www.iso.org/iso/home/store/catalogue_tc/catalogue_detail.htm?csnumber=70603,.

[32] Anke Vollertsen et al. "STANDARDIZED, MODULAR MICROFLUIDIC BUILDING BLOCKS FOR AUTOMATED CELL CULTURING SYSTEMS". In: ().

[33] Elsbeth G B M Bossink et al. "Multiplexed Organ-on-Chips with integrated macro valves for automated cell culture". In: *research.utwente.nl* (). URL: https://research.utwente.nl/files/275238899/PG1385.pdf.

[34] *ISO - IWA 23:2016 - Interoperability of microfluidic devices — Guidelines for pitch spacing dimensions and initial device classification.* URL: https://www.iso.org/standard/70603.html.

[35] David J. Guckenberger et al. "Micromilling: A method for ultra-rapid prototyping of plastic microfluidic devices". In: *Lab on a chip* 15.11 (June 2015), p. 2364. ISSN: 14730189. DOI: 10.1039/C5LC00234F. URL: /pmc/articles/PMC4439323/%20/pmc/articles/PMC4439323/?report=abstract%20https://www.ncbi.nlm.nih.gov/pmc/articles/PMC4439323/.

[36] *Lab-scale membrane systems, Microfluidic and customized systems Convergence Industry B.V.* URL: https://www.convergence.com/?gclid=Cj0KCQjw29CRBhCUARIsAOboZbJT1U6se5FsBsVtkos344xFQDsbsQ_ssx6LO9Aq0WpxAu8OFPSQGwUaAvfOEALw_wcB.

[37] *What is LabVIEW? - NI.* URL: https://www.ni.com/nl-nl/shop/labview.html.

[38] Guillermo J. Silva, Aniruddha Datta, and S. P. Bhattachaiyya. "PID Controllers for Time-Delay Systems". In: *PID Controllers for Time-Delay Systems* (2005). DOI: 10.1007/B138796.

[39] Johannes Schindelin et al. "Fiji: an open-source platform for biological-image analysis". In: *Nature methods* 9.7 (July 2012), pp. 676–682. ISSN: 1548-7105. DOI: 10.1038/NMETH.2019. URL: https://pubmed.ncbi.nlm.nih.gov/22743772/.

[40] *Fluigent - Smart Microfluidics - For research and industry.* URL: https://www.fluigent.com/.

[41] Iago Pereiro et al. "Nip the bubble in the bud: a guide to avoid gas nucleation in microfluidics". In: *Lab on a Chip* 19.14 (July 2019), pp. 2296–2314. ISSN: 1473-0189. DOI: 10.1039/C9LC00211A. URL: https://pubs.rsc.org/en/content/articlehtml/2019/lc/c9lc00211a%20https://pubs.rsc.org/en/content/articlelanding/2019/lc/c9lc00211a.

[42] Subhra Datta and Sandip Ghosal. "Characterizing Dispersion in Microfluidic Channels". In: *Lab on a chip* 9.17 (2009), p. 2537. ISSN: 14730189. DOI: 10.1039/B822948C. URL: /pmc/articles/PMC2814782/%20/pmc/articles/PMC2814782/?report=abstract%20https://www.ncbi.nlm.nih.gov/pmc/articles/PMC2814782/.

[43] S. Devasenathipathy and J. G. Santiago. "Electrokinetic Flow Diagnostics". In: *Microscale Diagnostic Techniques* (2005), pp. 113–154. DOI: 10.1007/3-540-26449-3{_}3. URL: https://link.springer.com/chapter/10.1007/3-540-26449-3_3.

[44] Albert Van Den Berg et al. "Fundamentals of microfluidic cell culture in controlled microenvironments". In: *Chemical Society Reviews* 39.3 (Feb. 2010), pp. 1036–1048. ISSN: 14604744. DOI: 10.1039/B909900J. URL: https://pubs.rsc.org/en/content/articlehtml/2010/cs/b909900j%20https://pubs.rsc.org/en/content/articlelanding/2010/cs/b909900j.

[45] *Formation of Uniform and Reproducible 3D Cancer Spheroids in High-Throughput Plates — Thermo Fisher Scientific - NL.*
URL: https://www.thermofisher.com/nl/en/home/references/newsletters-and-journals/bioprobes-journal-of-cell-biology-applications/bioprobes-72/bioprobes-72-3d-cancer-spheroids.html.

[46] C. R. Culy, D. Clemett, and L. R. Wiseman. "Oxaliplatin: A review of its pharmacological properties and clinical efficacy in metastatic colorectal cancer and its potential in other malignancies".
In: *Drugs* 60.4 (Sept. 2000), pp. 895–924. ISSN: 00126667.
DOI: 10.2165/00003495-200060040-00005/FIGURES/3.
URL: https://link.springer.com/article/10.2165/00003495-200060040-00005.

[47] *How Does Chemo Work? — Types of Chemotherapy.*
URL: https://www.cancer.org/treatment/treatments-and-side-effects/treatment-types/chemotherapy/how-chemotherapy-drugs-work.html.

[48] Shuanglian Li et al. "Role of organic cation transporter 1, OCT1 in the pharmacokinetics and toxicity of cis-diammine(pyridine)chloroplatinum(II) and oxaliplatin in mice".
In: *Pharmaceutical Research* 28.3 (Mar. 2011), pp. 610–625. ISSN: 07248741.
DOI: 10.1007/S11095-010-0312-6.

Appendices

A Convergence Inspector software

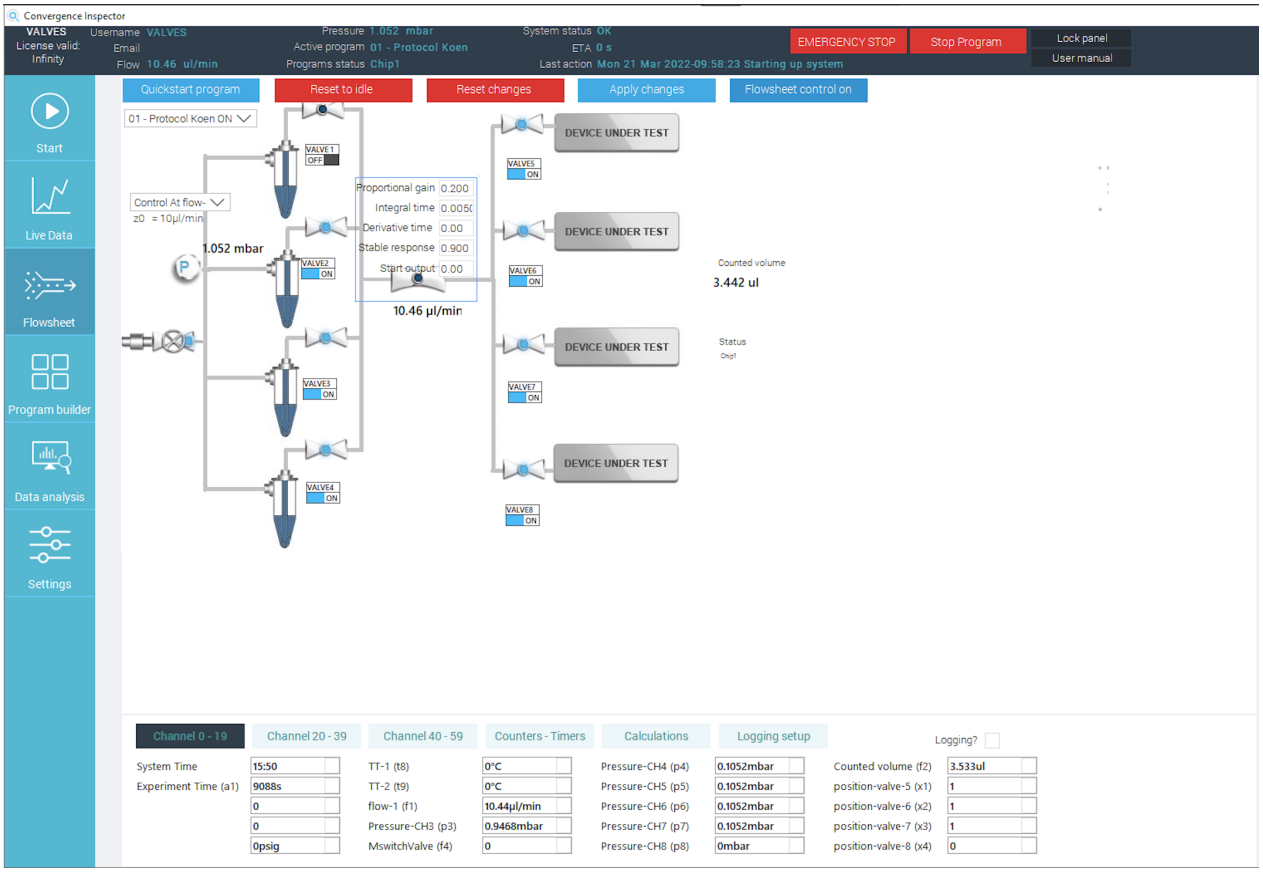

Figure 33: Overview of the Convergence Inspector software interface. With the tabs on the left side (start, live data, flowsheet, program builder, data analysis and settings) different menus can be selected. The flowsheet menu is shown here, where the function blocks in the schematic overview of the system control the opening/closing of valves, the set flow rate or pressure and the settings of the PID flow rate controller. Moreover, from this menu the desired protocol can be ran by pressing 'Quickstart program'.

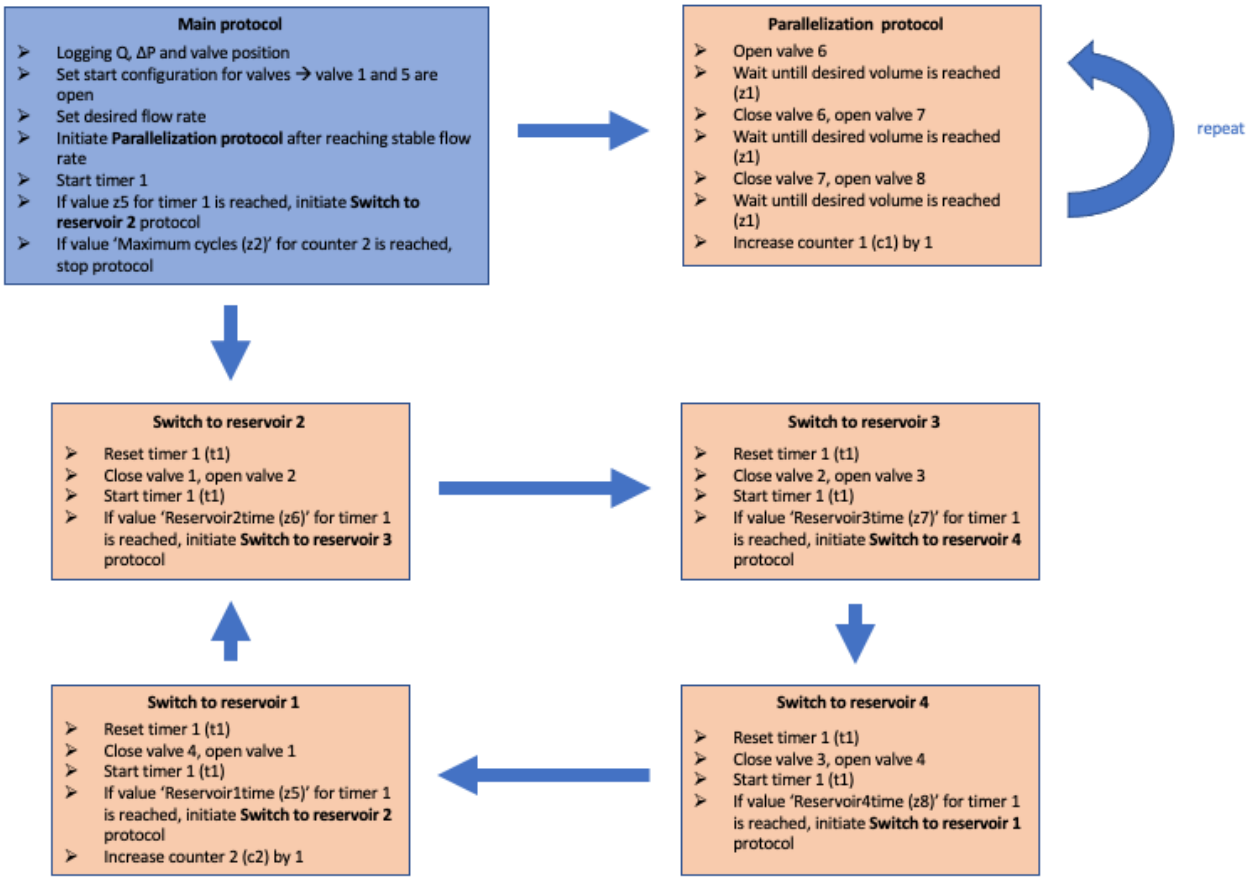

Figure 34: Schematic overview of the main program (blue) and sub-programs, where the actions performed by each (sub-)program is indicated inside the box.

B Tubing specifics of the setups

B.1 Sequential parallelization of flow

B.1.1 Commercially available equipment

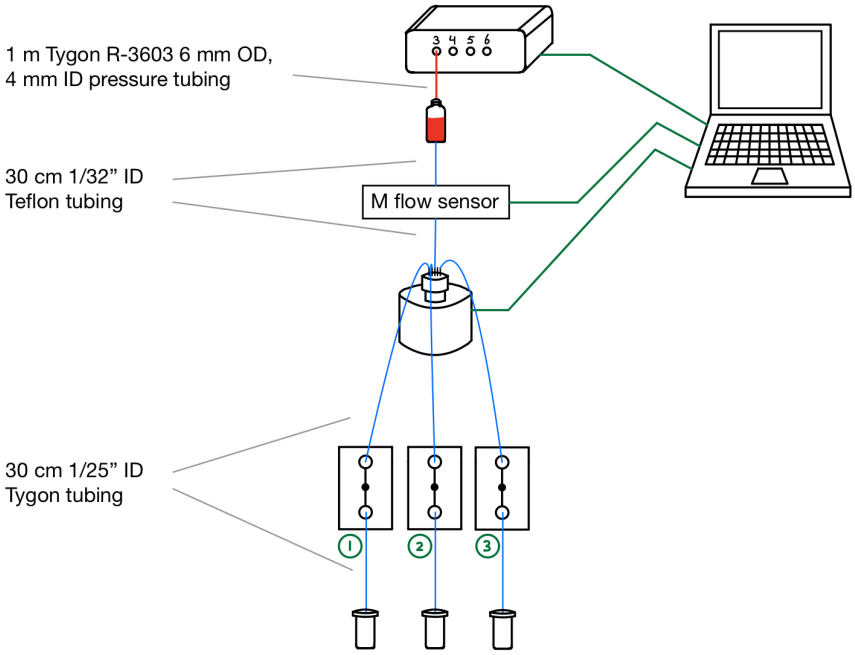

Figure 35: Specific tubing used in the setup for sequential parallelization with commercially available equipment.

B.2 Microfluidic chips on the TOP platform

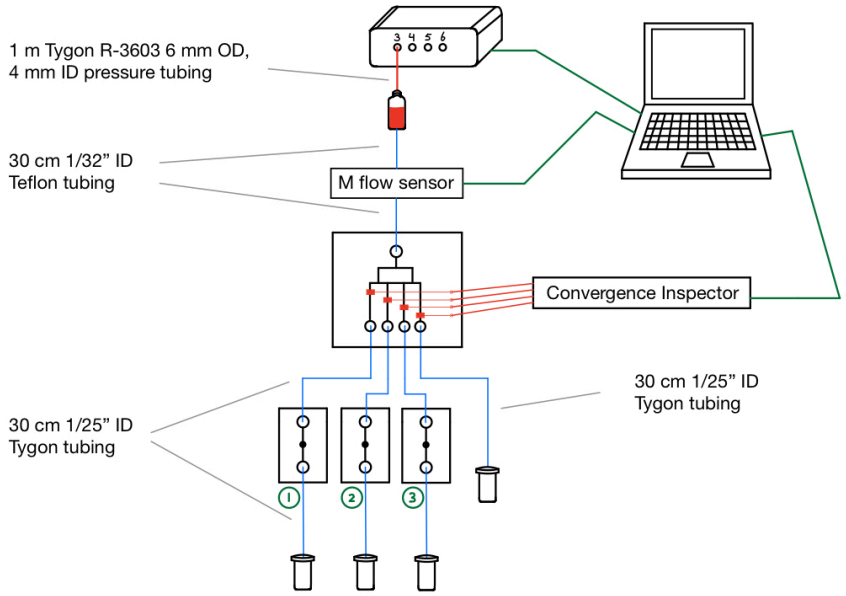

Figure 36: Specific tubing used in the setup for sequential parallelization with microfluidic chips.

B.3 Generating dynamic concentration profiles on chip

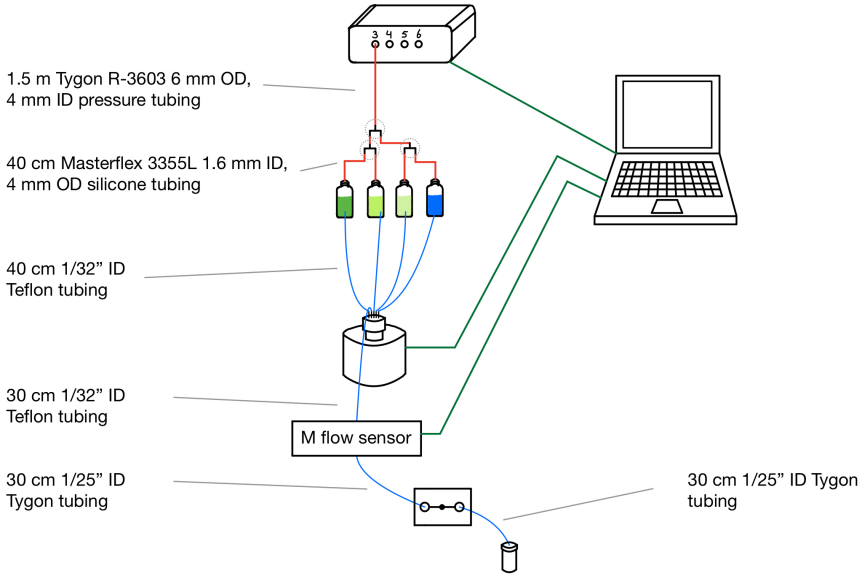

Figure 37: Specific tubing used in the setup for generating a dynamic fluorescein concentration profile on chip.

B.4 Integrating parallelization and dynamic drug concentration profiles

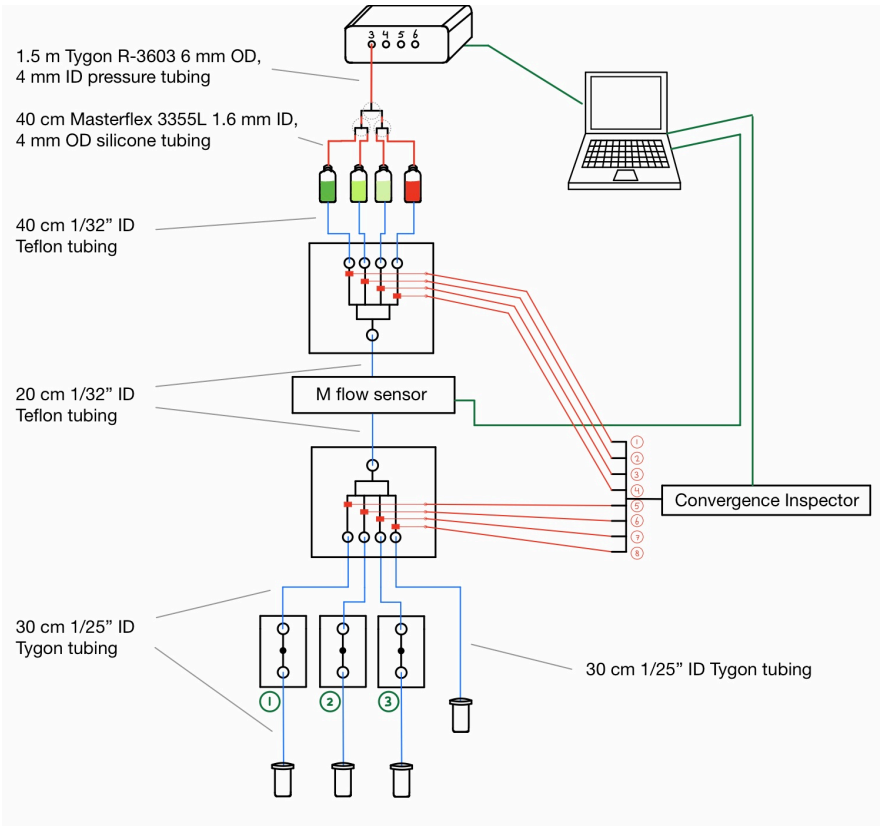

Figure 38: Specific tubing used for the system that was designed throughout this project

C Parallelization of the dynamic *in vivo* oxaliplatin concentration profile

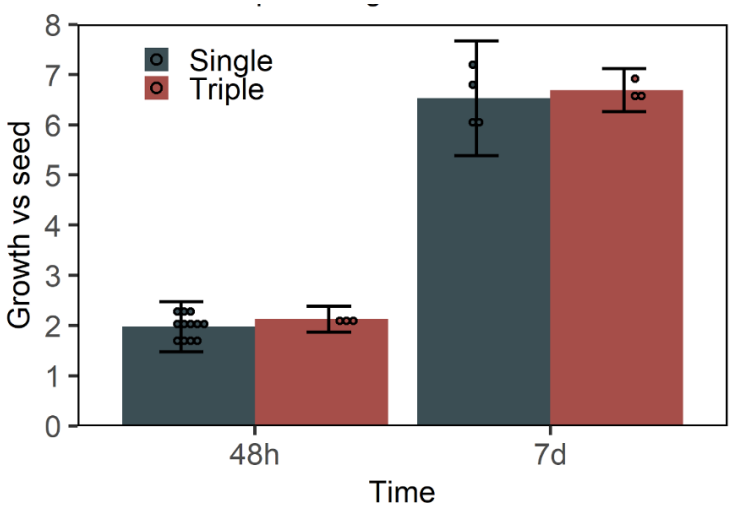

Figure 39: The growth of spheroids (HCT-116) at t = 48 h and t = 7 d, exposed to a continuous flow of cell culture medium at a flow rate of 2 µL/min. Cells were seeded four days in advance to the experiment with a seeding density of 2.000 cells per well.

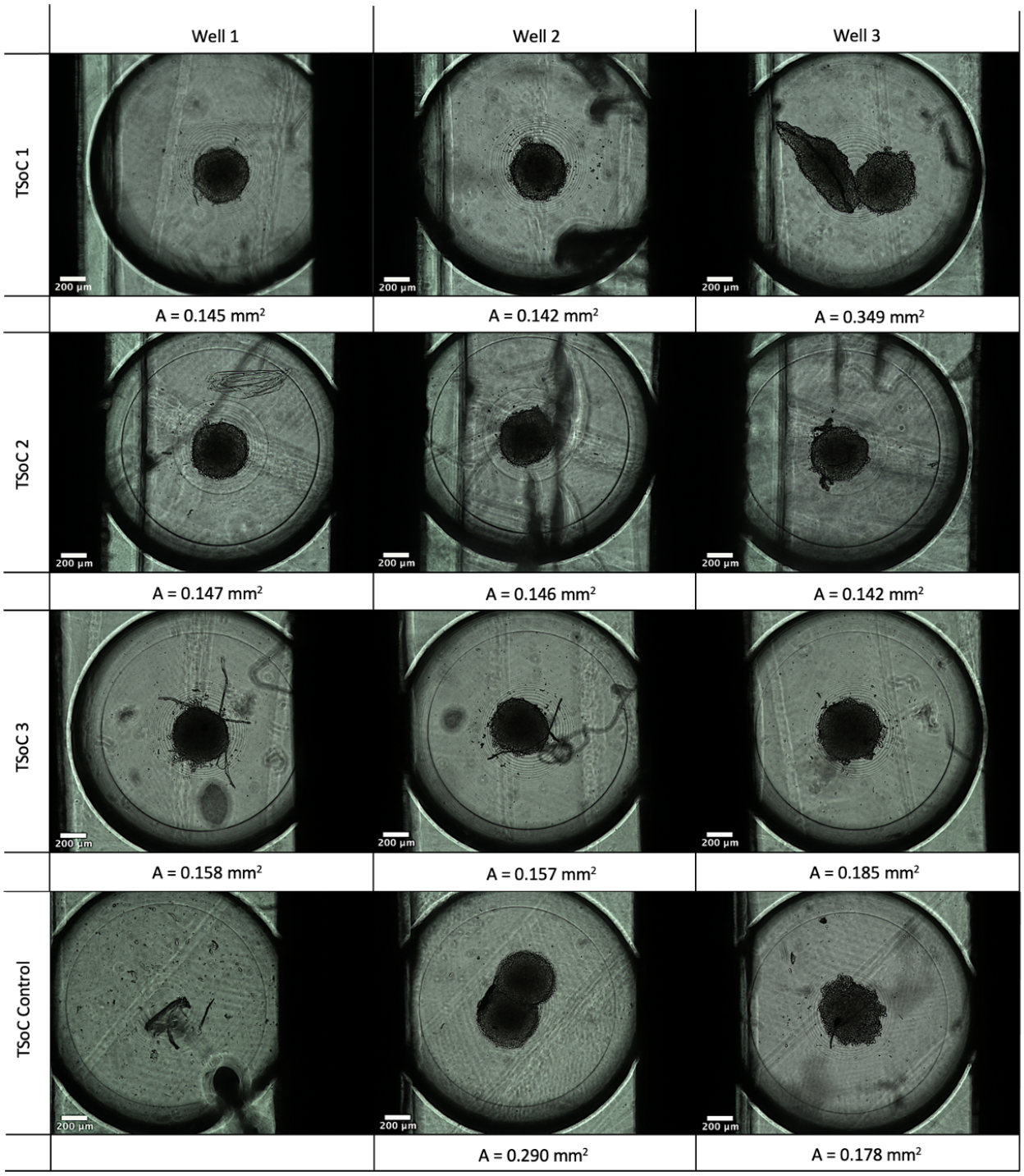

Figure 40: Images of the spheroids (HCT-116) on TSoC 1, 2 and 3 and control at t = 0 h. For each spheroid, the surface area is given in mm^2. Scale bar is 200 µm.